Computers in Biology and Medicine 105 (2019) 125–143

Contents lists available at ScienceDirect

Computers in Biology and Medicine

journal homepage: www.elsevier.com/locate/compbiomed

Performance evaluation of 10-year ultrasound image-based stroke/cardiovascular (CV) risk calculator by comparing against ten conventional CV risk calculators: A diabetic study

Narendra N. Khanna[a], Ankush D. Jamthikar[b], Deep Gupta[b], Andrew Nicolaides[c], Tadashi Araki[d], Luca Saba[e], Elisa Cuadrado-Godia[f], Aditya Sharma[g], Tomaz Omerzu[h], Harman S. Suri[i], Ajay Gupta[j], Sophie Mavrogeni[k], Monika Turk[l], John R. Laird[m], Athanasios Protogerou[n], Petros P. Sfikakis[o], George D. Kitas[p], Vijay Viswanathan[q], Jasjit S. Suri[r,*]

[a] Department of Cardiology, Indraprastha APOLLO Hospitals, New Delhi, India
[b] Department of Electronics and Communication Engineering, VNIT, Nagpur, India
[c] Vascular Screening and Diagnostic Centre, University of Cyprus, Nicosia, Cyprus
[d] Division of Cardiovascular Medicine, Toho University, Tokyo, Japan
[e] Department of Radiology, University of Cagliari, Italy
[f] Department of Neurology, IMIM - Hospital del Mar, Barcelona, Spain
[g] Cardiovascular Medicine, University of Virginia, VA, USA
[h] Department of Neurology, University Medical Centre Maribor, Slovenia
[i] Brown University, Rhode Island, USA
[j] Department of Radiology, Weill Cornell Medicine, NY, USA
[k] Cardiology Clinic, Onassis Cardiac Surgery Center, Athens, Greece
[l] Neurology Dept., University Medical Centre Maribor, Maribor, Slovenia
[m] Heart and Vascular Institute, Adventist Health St. Helena, St Helena, CA, USA
[n] Department of Cardiovascular Prevention & Research Unit Clinic & Laboratory of Pathophysiology, National and Kapodistrian Univ. of Athens, Greece
[o] Joint Rheumatology Program, National Kapodistrian University of Athens Medical School, Greece
[p] Dudley Group NHS Foundation Trust, Dudley, United Kingdom
[q] MV Hospital for Diabetes and Professor M Viswanathan Diabetes Research Centre, Chennai, India
[r] Stroke Monitoring and Diagnostic Division, AtheroPoint™, Roseville, CA, USA

ARTICLE INFO

Keywords:
10-Year cardiovascular risk calculator
Conventional cardiovascular risk factors
Covariates
Carotid
Ultrasound
Image-based phenotypes
Integrated calculator AECRS1.0$_{10yr}$

ABSTRACT

Motivation: AtheroEdge Composite Risk Score (AECRS1.0$_{10yr}$) is an integrated stroke/cardiovascular risk calculator that was recently developed and computes the 10-year risk of carotid image phenotypes by integrating conventional cardiovascular risk factors (CCVRFs). It is therefore important to understand how closely AECRS1.0$_{10yr}$ is associated with the ten other currently available conventional cardiovascular risk calculators (CCVRCs).

Methods: The Institutional Review Board of Toho University approved the examination of the left/right common carotid arteries of 202 Japanese patients. Step 1 consists of measurement of AECRS1.0$_{10yr,}$ given current image phenotypes and CCVRFs. Step 2 consists of computing the risk score using ten different CCVRCs given CCVR factors: QRISK3, Framingham Risk Score (FRS), United Kingdom Prospective Diabetes Study (UKPDS) 56, UKPDS60, Reynolds Risk Score (RRS), Pooled cohort Risk Score (PCRS or ASCVD), Systematic Coronary Risk Evaluation (SCORE), Prospective Cardiovascular Munster Study (PROCAM) calculator, NIPPON, and World Health Organization (WHO) risk. Step 3 consists of computing the closeness factor between AECRS1.0$_{10yr}$ and ten CCVRCs using cumulative ranking index derived using eight different statistically derived metrics.

Results: AECRS1.0$_{10yr}$ reported the highest area-under-the-curve (**0.927**;$P < 0.001$) among all the risk calculators. The top three CCVRCs closest to AECRS1.0$_{10yr}$ were QRISK3, FRS, and UKPDS60 with cumulative ranking

* Corresponding author. Fellow AIMBE Diagnostic and Monitoring Division, AtheroPoint™, Roseville, Roseville, CA, 95661, USA.
E-mail address: jasjit.suri@atheropoint.com (J.S. Suri).

https://doi.org/10.1016/j.compbiomed.2019.01.002
Received 24 November 2018; Received in revised form 4 January 2019; Accepted 5 January 2019

scores of 2.1, 3.0, and 3.8, respectively.
Conclusion: AECRS1.0$_{10yr}$ produced the largest AUC due to the integration of image-based phenotypes with CCVR factors, and ranked at first place with the highest AUC. Cumulative ranking of ten CCVRCs demonstrated that QRISK3 was the closest calculator to AECRS1.0$_{10yr}$, which is also consistent with the industry trend.

1. Introduction

Cardiovascular diseases (CVD) including heart and stroke are the major cause of mortality and morbidity around the world [1]. The spread of CVD is almost similar in every region of the world including developed and developing countries [2,3]. Atherosclerosis is the primary cause of cardiovascular disease [4]. Coronary and carotid arteries are the main sources that supply the oxygenated blood to the heart and the brain, the two main organs that are responsible for heart attack and stroke. Deposition of atherosclerotic plaque within the vessel wall obstructs this blood supply causing myocardial infarction (MI) or stroke. According to INTERHEART[1] [5] and INTERSTROKE[1] [6] studies, 90% of the mortalities due to these CVD are attributed to the conventional cardiovascular risk (CCVR) factors such as age, ethnicity, systolic blood pressure (SBP), low-density lipoproteins cholesterol (LDL-C), total cholesterol (TC), smoking, diabetes mellitus (DM), and family history (FH). These risk factors have an additive effect on atherosclerotic vascular biomarkers causing an elevation in CVD/Stroke risk.

Preventive interventional methods (i.e., use of statins) require the determination of baseline as well as the long-term risk of a patient to prevent the onset of CVD. Risk estimation can be possible using cardiovascular (CV) risk calculators. From here on, we will use CCVRCs for "conventional cardiovascular risk calculators". At the present stage, there are more than 100 CCVRCs available [7]. Most prominently and clinically used CCVRCs are FRS [8], UKPDS56 [9], UKPDS60 [10], QRISK3 [11], RRS [12], NIPPON [13], SCORE [14], WHO [15], PCRS (Atherosclerosis CVD - ASCVD) [16], and PROCAM [17] (The expansions of the abbreviation is shown in Appendix-Table 1). This was the main motivation for using only these ten CCVRCs in this study to evaluate the performance of AECRS1.0$_{10yr}$ and to further study which calculator was most closely related to AECRS1.0$_{10yr}$. In this manuscript, the suffix '10yr' indicates the risk value after ten years. CCVR calculators generally provide a risk estimation based on traditional risk factors. Recent guidelines indicate the use of some primitive CV risk calculators to assess the 10-year risk of CVD and to decide the statin eligibility for the patients [18–20]. Although such CCVRCs can provide the basis for the prescription of statins (i.e., lipid-lowering medications) for treating the risk of CVD, they sometimes do the not explain the CV events due to the morphological variations in the atherosclerotic blood vessels. Furthermore, CCVR factors do not provide any information about the arterial plaque variations or their components. However, since CCVR factors contribute to the risk of stroke/coronary heart disease (CHD), they are also termed as risk factors.

Advancements in imaging techniques especially non-invasive imaging modalities such as carotid ultrasound provide a cost-effective tool to assist physicians in understanding the morphological variations of the blood vessels due to atherosclerotic plaque tissues [19,21]. For example, carotid intima-media thickness (cIMT) and total plaque area (TPA) are the two important image-based phenotypes of carotid atherosclerosis that can provide information about the cardiovascular health of patients [22–27] Note that there were a total of 28 CCVR factors considered in this study, and their abbreviations are all expanded in Appendix-Table 2. Since 2000, seven clinical guidelines have been recommended for using cIMT and/or carotid plaque for assisting the CVD risk estimation [28]. In 2010, Nambi et al. [29] demonstrated a significant improvement in CHD by taking into consideration the image-based phenotypes such as cIMT and carotid plaque. Stein et al. [30] also recommended the use of cIMT for CHD risk prediction. Polak et al. [31] presented a study with 296 participants and reported that CV outcomes can be predicted using the mean and the maximum cIMT. Association between intima-media thickness (IMT) in the common carotid artery (CCA) and coronary SYNTAX score was demonstrated by Ikeda et al. [32] in their study of 500 diabetic patients. The same group showed the link between carotid bulb plaques and coronary SYNTAX score in diabetic patients [33]. Recently, Suri et al. [34] showed the role of cIMT and variations in IMT (IMTV) to predict the Leukoaraiosis disease in adults. Thus, there is an additional benefit by considering the carotid image-based phenotypes in the risk prediction models along with CCVR factors for risk estimation.

Conventional cardiovascular risk calculators do not consider carotid image-based phenotypes in their risk prediction models. Therefore, the extent of atherosclerotic plaque measured using average intima-media thickness (IMT$_{ave}$), maximum IMT (IMT$_{max}$), minimum IMT (IMT$_{min}$), IMT variability (IMTV), and the morphology or echolucency [35] of the plaque (such as hyper- or hypo-echoic intensities of the grayscale images [36]) remains unexplained by such as CCVRCs. Note that both carotid plaque or wall thickening and CCVR factors are time (or age) dependent [37–39]. Thus, one can compute the 10-year risk of stroke/CVD by knowing the projection rates of the image-based phenotypes due to the conventional risk factors and then integrating them with current image-based phenotypes. These 10-year image-based phenotypes (such as IMT$_{ave10yr}$, IMT$_{max10yr}$, IMT$_{min10yr}$, and IMTV$_{10yr}$) lead to the formation of the overall risk or composite risk score (CRS). This is known as an integrated calculator, integrated in the sense that conventional risk factors are integrated or fused with image-based phenotypes. Since our image-based phenotypes, to begin with, were measured automatically using AtheroEdge (AE) system (AtheroPoint, Roseville, CA, USA), we call this composite risk score as AECRS1.0$_{10yr}$.

The main objective of the study is to evaluate AECRS1.0$_{10yr}$ (an integrated stroke/CV risk calculator) by comparing against the 10-year CCVRCs using several statistical metrics. The theory of these metrics is to evaluate the metric criteria given the CCVR factors for each patient corresponding to these eleven CV risk calculators (ten CCVRCs and the integrated calculator - AECRS1.0$_{10yr}$). These metrics are either based on how well the CCVR calculators find the high-risk patients in terms of similarity with AECRS1.0$_{10yr}$ (so-called, similarity metric represented by a metric type of M1), or how far AECRS1.0$_{10yr}$ is from the ten CCVR calculator constellations or cluster (clustering metric represented by a metric type of M2), or how the overall cohort of patients (or population) is doing in terms of its precision when compared against AECRS1.0$_{10yr}$ (precision-of-merit metric represented by a metric type of M3), or ability to find the mean statistics for all CCVRCs against AECRS1.0$_{10yr}$ (figure-of-merit metric represented by a metric type of M4), or how each patient's risk in CCVRC deviates against AECRS1.0$_{10yr}$ (metric-type M5), or how each patient's risk in AECRS1.0$_{10yr}$ deviates against CCVRC (metric-type of M6), or adapt kappa statistics to see the disparity between readings (kappa metric-type of M7), or the ability to use logistic regression and rank CCVRCs using odds ratio against AECRS1.0$_{10yr}$ (metric-type M8). The overall idea is to understand which CCVRC is ranked closer to the AECRS1.0$_{10yr}$. The list of the eight statistical metrics and expansion of the abbreviations and symbols pertaining to performance metrics are listed in Appendix-Table 3 and Appendix-Table 4, respectively.

There are two hypotheses in this study: (i) The calculator which has a direct impact on atherosclerosis disease should show the highest area-

[1] As it is taken from the Rosengren et al. and O'Donnell et al.

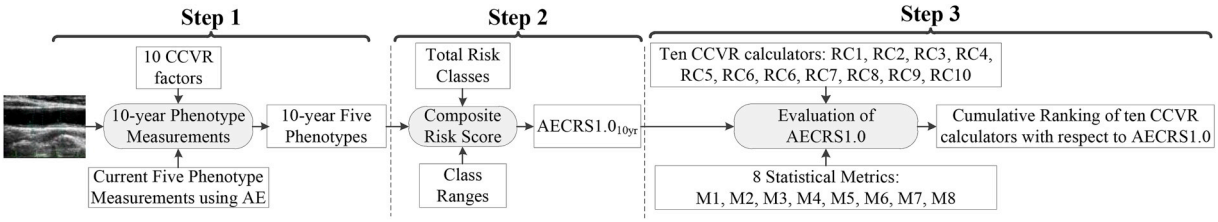

Fig. 1. Performance evaluation of AECRS1.0$_{10yr}$ against ten CCVR calculators. Ten risk calculator are RC1:FRS, RC2:UKPDS56, RC3:UKPDS60, RC4:RRS, RC5:PCRS, RC6:SCORE, RC7:NIPPON, RC8:QRISK3, RC9:PROCAM, and RC10:WHO risk charts. Eight statistical metrics are M1: similarity index, M2: clustering method, M3: precision-of-merit, M4: figure-of-merit, M5: deviation of CCVR calculator from mean AECRS1.0$_{10yr}$, M6: deviation of AECRS1.0$_{10yr}$ from mean CCVR calculator, M7: kappa coefficient, and M8: logistic regression and ROC analysis.

under-the-curve (AUC) and (ii) we believe that the calculator that uses a larger number of CCVR factors is likely to be closer to the AECRS1.0$_{10yr}$ risk calculator, since AECRS1.0$_{10yr}$ is an integrated calculator. Our current study has several novelties: (i) a carotid ultrasound image-based phenotypes 10-year risk prediction model called AECRS1.0$_{10yr}$ has been proposed; (ii) performance of AECRS1.0$_{10yr}$ was evaluated against CCVRCs (Fig. 1); and (iii) a novel performance evaluation scheme consisting of eight statistical metrics has been proposed to compare the closeness of AECRS1.0$_{10yr}$ against the ten CCVRCs.

The layout of the paper is as follows. Section 2 discusses the study population and image acquisition protocol. The methodology for the measurements of carotid image-based phenotypes has been discussed in section 3. The statistically derived metrics for evaluating the closeness factor between AECRS1.0$_{10yr}$ and CCVR calculators have been presented in section 4. Results are presented in section 5. Discussion and benchmarking have been discussed in section 6. The paper concludes in section 7.

2. Study population and image acquisition

2.1. Study population

Between July 2009 and December 2010, a Japanese cohort of 202 patients was recruited from Toho University, Japan (Approved by the Institutional Review Board) and written consents were taken from all the participants. A total of 404 B-Mode ultrasound scans were collected from both left and right CCA. The scans were retrospectively analyzed by two operators (novice and experienced) as well as an expert who had 15 years of experience in the field of radiology. This study presents a unique and novel vision, design of novel algorithms, and comprehensive statistical data analysis compared to previous studies that published the same Japanese cohort [26,40–43]. The baseline characteristics of this cohort are presented in the result section.

2.2. Ultrasound image acquisition

Carotid arteries for 202 patients were examined using an ultrasound scanner (Aplio XG, Xario, Aplio XV, Toshiba Inc., Tokyo, Japan). A total of 404 B-mode ultrasound images were acquired by a skilled sonographer with 15 years of experience in ultrasonography. The detailed acquisition protocol has already been discussed in the previous study published by our group [44]. Overall average resolution factor for all the B-mode ultrasound scans was 0.0529 mm-per-pixel. The guidelines of American Society of Echocardiography Carotid Intima-Media Task Force 16 were adopted in this study [28].

3. Methodology for composite risk score for integrated calculator

Our scheme of evaluation of an integrated calculator AECRS1.0$_{10yr}$ is based on several metrics whose fundamental assumption is to examine which of the popular ten CCVRCs is closest to AECRS1.0$_{10yr}$. This requires three important components: (a) computation of AECRS1.0$_{10yr}$; (b) risk computation from the ten CCVRCs (RC1 to RC10, here RC indicates the risk calculator), and (c) design of the eight metrics (M1 to M8) which were used for evaluation of AECRS1.0$_{10yr}$. A brief description of the system is presented in Fig. 1. Step 1 deals with 10-year predictions of carotid ultrasound image-based phenotypes by fusing the ten CCVR factors and five automated image-based phenotypes [45]. Step 2 consists of computing the composite risk score, AECRS1.0$_{10yr}$, given the 10-year image-based phenotypes, class ranges and total risk classes. In Step 3 (the main innovation of this study), eight statistical metrics (labeled as M1 to M8) were used to investigate the closeness between the ten risk CCVRCs (labeled as RC1 to RC10) and AECRS1.0$_{10yr}$. Step 1 and step 2 are briefly discussed in this study since it has been presented before. Section 3.1 presents the automated image phenotype measurements, section 3.2 presents the 10-year image-based phenotypes given the CCVR factors and section 3.3 presents the computation of AECRS1.0$_{10yr}$.

3.1. Carotid ultrasound image-based phenotype measurement

Intima-media thickness (IMT) and morphologic total plaque area (mTPA) are the important carotid ultrasound image-based phenotypes. Four different types of IMTs such as IMT$_{ave}$, IMT$_{max}$, IMT$_{min}$, and IMTV were extracted from the far wall of the carotid ultrasound image of the CCA [26,46]. All of the five phenotypes, including mTPA, were extracted using an automated system (AtheroEdge from AtheroPoint™, Roseville, CA, USA) [46–49]. The mTPA is defined as the focal thickening of one mm above the baseline distance between the lumen-intima (LI) and media adventitia (MA) borders of the far wall of the CCA [50,51]. In this study, we refer “mTPA” as “TPA” because both of these two terms have equal meanings. The protocol for acquiring the automated measurements of the carotid ultrasound images-based phenotypes has already been discussed in our previous studies [46–48]. Five automated image-based phenotypes were also validated against manual analysis (the gold standard in this case) and computed tomography [52,53].

The annual progressions of cIMT and TPA are also influenced by the variations in CCVR factors [54–57]. Thus, in order to combine the effect of CCVR factors on imaging phenotypes, five types of 10-year phenotypes (IMT$_{ave10yr}$, IMT$_{max10yr}$, IMT$_{min10yr}$, IMTV$_{10yr}$, and TPA$_{10yr}$) were developed by fusing current image-based phenotypes (IMT$_{ave}$, IMT$_{max}$, IMT$_{min}$, IMTV, and TPA) with the ten CCVR factors (Age, Ethnicity, Artery type, Gender, TC, LDL-C, SBP, Smoking, glycated hemoglobin (HbA1c), and body mass index (BMI)) [45].

3.2. Composite risk score: AECRS1.0$_{10yr}$

Our carotid ultrasound image-based phenotype risk score is called AECRS1.0$_{10yr}$ and was used in this study to predict the 10-year CV risk on a Japanese cohort. The proposed AECRS1.0$_{10yr}$ was based on the composite risk computed using five 10-year carotid ultrasound image-based phenotype measurements (IMT$_{ave10yr}$, IMT$_{max10yr}$, IMT$_{min10yr}$, IMTV$_{10yr}$, and TPA$_{10yr}$). The complete development process of

AECRS1.0_{10yr} is also depicted in Fig. 1 in an "Introduction" section.

3.3. Conventional cardiovascular risk calculators

In order to validate the performance of the AECRS1.0_{10yr}, the 10-year CV risk was also computed using ten CCVRCs such as the FRS [8], the UKPDS56 [9], the UKPDS60 [10], the PCRS (also called as ASCVD score), the NIPPON [13], the RRS [12], the SCORE [14], the World Health Organization/International Society of Hypertension (WHO/ISH) risk charts, the PROCAM calculator [17], and the QRISK3 [11] using well established mathematical expressions [8–13,16]. Each of the CCVRCs uses a different set CCVR factors (See Appendix-Table 5). For example, UKPDS60 used six risk factors without using HbA1c in its risk prediction model [10]. NIPPON used six CCVR factors including glucose tolerance level [13]. Similarly, PROCAM used eight CCVR factors including high-density lipoprotein cholesterol (HDL-C), family history, and triglyceride, which were not part of the UKPDS56 model [9,17]. Our study did not have all the CCVR factors required by each of the ten CCVRCs. All the risk factors which were not part of the Japanese cohort were not included in the 10-year risk computation using these ten CCVRCs.

3.4. Statistical analysis

Statistical analysis was performed using SPSS version 23 and validated using MATLAB 2017b. All the statistical variables were expressed in mean ± SD. As per the power analysis with standard normal distribution reflecting 95% confidence interval and 5% error margin, a sample size of 334 was expected. In this study, 21% more than the expected samples have been used (404 ultrasound scans). Thus, as per our power analysis, the recruited sample size was sufficient to perform all the statistical analysis.

4. Metrics for evaluating AECRS1.0_{10yr} against ten CCVRCs

The main contribution of this study is to evaluate the AECRS1.0_{10yr} by comparing against the ten popular CCVRCs. The design of these metrics is based on the closeness of the ten unique clusters representing the ten different CCVRCs to the integrated AECRS1.0_{10yr}. The design of the metrics provides full coverage in every way by leveraging on statistics to define this closeness. This full coverage means that we investigate the closeness or ranking of ten CCVRCs w.r.t AECRS1.0_{10yr} by considering distances, mean deviations, cluster centers, and a combination of statistical measures which can order the calculators using odds ratio. Keeping this in mind, given the risk values of 404 images for each of the ten CCVRCs (i.e., $404 \times 10 \sim 4040$ risk values) and the corresponding 404 AECRS1.0_{10yr} values, we approach these metric designs in the sections below (Appendix-Table 4 shows the abbreviation table pertaining to performance metrics, while Appendix-Table 6 shows the symbols pertaining to performance evaluation):

4.1. Metric 1: similarity index between AECRS1.0_{10yr} and ten CCVR calculators

The concept behind this algorithm is to investigate what percentage of the same high-risk patients overlap between two calculators given corresponding thresholds of the risk calculators. This tells the two calculators' ability to find the common patients between two pools: AECRS1.0_{10yr} and CCVRC. The common set of patients can then be computed using the similarity measure or index and converted into representation as a percentage. Computation of the similarity index (SI) between two calculators is a four-step process: (i) *Risk Stratification:* all patients were risk stratified into the high-risk or low-risk class using 11 CV risk calculators, which include AECRS1.0_{10yr} and the ten CCVRCs; (ii) *Similarity Count:* all similar patients who were risk-stratified into the high-risk class using both AECRS1.0_{10yr} and each of the ten CCVRCs were noted to obtain ten different similarity counts; (iii) *Threshold Variation:* step 1 and 2 were repeated for all the classification risk thresholds which were obtained by varying it between 1% and 5%, in an increment of 1%; and (iv) *Statistics Collection:* Mean value and standard deviation of the similarity index was then computed by averaging all the similarity counts taken over the range of risk thresholds. The above four steps of similarity index computation between AECRS1.0_{10yr} and each of the ten CCVRCs was computed and expressed as Mean ± SD. The symbolic representation for the computation process has been presented below.

Let A_t be a set of risk values for the patients corresponding to the risk calculator: AECRS1.0_{10yr} and the risk value are represented as high or low (1 or 0). Similarly, let B_t be a set of risk values for the patients corresponding to the CCVRCs and the risk value are represented as high or low (1 or 0). Thus these sets can be mathematically represented as: $A_t = [a_1^t, a_2^t, \ldots a_N^t]$ and $B_t = [b_1^t, b_2^t, \ldots b_N^t]$, N is the total number of images in the cohort. Further, these sets are for the specific risk threshold 't'. The objective of this algorithm is to find total samples in both sets which have high-risk values. Mathematically, this can be given as: $\forall\ a_i^t \in A_t$ and $\forall\ b_j^t \in B_t$, find the total elements in set A_t and B_t when $a_i^t = b_j^t$. The total number of elements which are common in these two sets is the similarity count. Note that this is specifically for one threshold value 't'. This is repeated for all the threshold values within a tolerance of 5% and a similarity counts were computed.

Consider S(t) be the SC corresponding to the global risk threshold value of "t". In order to compute the SI, the global risk threshold "t" was varied from −5% to +5% in the increment of 1%. Thus, we obtained ten different values for the risk thresholds. Let, T be the total number of risk thresholds i.e., T = 10. For each of these ten thresholds, SC was computed. Thus, the set of SC for T thresholds will be given as S(k), where k changes from 1 to 10. Finally, a mean and standard deviation of all the T similarity counts will be computed to obtain the SI between AECRS1.0_{10yr} and $CCVRC_n$. Note that $CCVRC_n$ is the nth CCVRC among the set of ten. The mean SC between AECRS1.0_{10yr} and $CCVRC_n$ for all the T thresholds is given as, $\mu_S(CCVRC_n, AECRS1.\ 0_{10yr}) = \frac{1}{T}(\sum_{k=1}^{T} S(k))$. Corresponding standard deviation is computed as: $\sigma_s(CCVRC_n, AECRS1.\ 0_{10yr}) = \sqrt{\left(\frac{\sum_{k=1}^{T}(S(k) - \mu_S(CCVRC_n, AECRS1.0_{10yr}))^2}{T-1}\right)}$. The SI between AECRS1.$0_{10yr}$ and $CCVRC_n$ will be then expressed as $SI(CCVRC_n, AECRS1.\ 0_{10yr}) = \mu_S(CCVRC_n, AECRS1.\ 0_{10yr}) \pm \sigma_s(CCVRC_n, AECRS1.\ 0_{10yr})$. The entire process of SI computation will be then repeated for all the ten CCVRCs.

4.2. Metric 2: clustering-based ranking method for ten CCVR calculators

The main concept in this metric is to find the closeness of a CCVRC to AECRS1.0_{10yr} by taking the entire cluster framed using the cohort. We look for the central tendency of the cluster by finding the center-of-mass of the cohort. The minimum Euclidean distance between the two cluster centers is a direct measure of their closeness. Thus, the algorithm of this clustering-based architecture consists of the following steps: (i) Risk computation: This step computes the risk values using AECRS1.0_{10yr}, and the conventional cardiovascular risk calculator; (ii) Center-of-Mass (CoM) computation: Given the risk values for all the samples of the cohort, this step uses the moment-of-inertia paradigm for computation of CoM representing the cluster. The CoM coordinates were mathematically computed as: $x_{CoM} = \left[\frac{\sum_{i=1}^{N}(x_i \times y_i)}{\sum_{i=1}^{N} y_i}\right]$ and $y_{CoM} = \left[\frac{\sum_{i=1}^{N}(x_i \times y_i)}{\sum_{i=1}^{N} x_i}\right]$, where, x_i is the risk value from the calculator under consideration and y_i is the risk factor under consideration corresponding to the ith ultrasound scan, respectively. N is the total number of ultrasound scans of the cohort. The variable "y" takes four different possibilities such age, TC, HbA1c, and SBP. The CoM value is computed for both AECRS1.0_{10yr} and CCVR calculator. This leads us to

computation of (x,y) pairs for AECRS1.0_{10yr} and CCVR calculator; (iii) Step 3: Euclidean distance (ED): This step involves computation of the minimum ED between the two CoMs computed for AECRS1.0_{10yr} and CCVRC. Let us consider the CoM for AECRS1.0_{10yr} is represented as $(x_{CoM}^{AECRS1.0_{10yr}}, y_{CoM}^{AECRS1.0_{10yr}})$ and CoM for $CCVRC_n$ is represented as $(x_{CoM}^{CCVRC_n}, y_{CoM}^{CCVRC_n})$. The ED between CoMs of AECRS1.0_{10yr} and CCVR calculator is mathematically expressed as, $ED = \sqrt{(x_{CoM}^{AECRS1.0_{10yr}} - x_{CoM}^{CCVRC_n})^2 + (y_{CoM}^{AECRS1.0_{10yr}} - y_{CoM}^{CCVRC_n})^2}$; (iv) ED array for the chosen risk factor: repeat all the three steps by using all the CCVRCs: RC1 to RC10 and compare against AECRS1.0_{10yr} to generate the array of EDs; (v) Closest risk calculator: This step estimates which conventional calculator's cluster center is closest ito AECRS1.0_{10yr} cluster center $(x_{CoM}^{AECRS1.0_{10yr}}, y_{CoM}^{AECRS1.0_{10yr}})$; and (vi) Cluster vs. risk factor plot: Repeat steps 1 to 5 by changing the risk factor and plot the cluster centers for ten calculators corresponding to all the risk factors. The cluster center (taken from the conventional calculators) closed to the AECRS1.0_{10yr} cluster center represents the closest. In this protocol, the four exemplary risk factors were selected which influences the atherosclerotic wall directly or indirectly using CCVR factors. This includes age, TC (as part of lipid variation), HbA1c (due to DM), and SBP (due to hypertension).

4.3. Metric 3: precision-of-merit between AECRS1.0_{10yr} and ten CCVR calculators

Precision-of-merit (PoM) investigates the precise closeness between the risk measurements computed using AECRS1.0_{10yr} and the ten CCVR calculators. It was computed by considering the mean absolute error (MAE) between AECRS1.0_{10yr} and the ten CCVR calculators. Mathematically, PoM is represented as $PoM_n = 100 - MAE_n$, where MAE_n is given as $MAE_n = \left[\frac{1}{N} \times \sum_{i=1}^{N} \left(\frac{|AECRS1.0_{10yr}(i) - CCVR_n(i)|}{AECRS1.0_{10yr}(i)}\right)\right] \times 100$, where $CCVR_n(i)$ and AECRS1. $0_{10yr}(i)$ represents the risk values for the i^{th} ultrasound scan corresponding to nth risk calculator and AECRS1. 0_{10yr}. N is the total number of ultrasound scans (i.e., 404 B-mode images) and the ratio $\left(\frac{|AECRS1.0_{10yr}(i) - CCVR_n(i)|}{AECRS1.0_{10yr}(i)}\right)$ indicates the absolute difference between the risk values corresponding to the risk calculators AECRS1. $0_{10yr}(i)$ and $CCVR_n(i)$. This computation is repeated between AECRS1.0_{10yr} and the ten CCVRCs by changing "n" from 1 to 10. Finally, the PoM_n is ranked in ascending order to investigate the closeness between CCVRCs and AECRS1.0_{10yr}.

4.4. Metric 4: figure-of-merit between AECRS1.0_{10yr} and ten CCVR calculators

Similar to PoM, figure-of-merit (FoM) is another metric that investigates the closeness between AECRS1.0_{10yr} and ten CCVRCs. This metric provides a broad view of the overall performance of two calculators by comparing their average risk values. Since it takes into consideration only the first moment of two calculators (AECRS1.0_{10yr} and CCVRC), it is computationally efficient. Given average CV risk values computed using AECRS1.0_{10yr} ($\overline{AECRS1.0}_{10yr}$) and nth CCVRC ($\overline{CCVR}_n$) under consideration, FoM is mathematically expressed as $FoM = 100 - \left[\left(\frac{|\overline{AECRS1.0}_{10yr} - \overline{CCVR}_n|}{\overline{AECRS1.0}_{10yr}}\right) \times 100\right]$, where $\overline{AECRS1.0}_{10yr} = (\frac{1}{N} \times \sum_{i=1}^{N} AECRS1.\ 0_{10yr}(i))$ and $\overline{CCVR}_n = (\frac{1}{N} \times \sum_{i=1}^{N} CCVR_n(i))$. AECRS1. $0_{10yr}(i)$ and $CCVR_n(i)$ are the 10-year CV risk values for the ith ultrasound scan. Similar to POM, the ten FoM values corresponding to the ten CCVRCs were computed and ranked in an ascending order to investigate the degree-of-closeness between AECRS1.0_{10yr} and ten CCVRCs.

4.5. Metric 5 & 6: ranking method based on the deviation from mean

Two types of ranking were performed using the "deviation from mean" method. This concept helps in determining the deviation of all the risk values from calculator one compared to the mean of the calculator two. This is also called in simpler terms as the mean absolute deviation (MAD). There are two classes of calculators: CCVRCs and AECRS1.0_{10yr}. Since there are "B" CCVRCs, then there are 2xB possibilities of MAD:

(i) Deviation of $CCVRC_n$ from $\overline{AECRS1.0}_{10yr}$ or Mean Absolute Deviation (MAD): Mean absolute deviation was taken between the CCVRC and the mean of AECRS1.0_{10yr}. If $CCVRC_n(i)$ represents the risk value of the nth CCVRC for the i^{th} ultrasound scan, and $\overline{AECRS1.0}_{10yr}$ is the mean of the risk values over N ultrasound scans (i.e., 404 scans), then MAD of $CCVRC_n$ against $\overline{AECRS1.0}_{10yr}$ is mathematically represented as:

$$MAD^N(CCVRC_n, \overline{AECRS1.0}_{10yr}) = \frac{1}{N} \sum_{i=1}^{N} |(CCVRC_n(i) - \overline{AECRS1.0}_{10yr})| \quad (1)$$

(ii) Deviation of AECRS1.0_{10yr} from $\overline{CCVRC}_n$: Mean Absolute Deviation (MAD): Similarly, in the second method, the mean absolute deviation was computed between AECRS1.0_{10yr} and the mean of all the ten CCVR calculators, $\overline{CCVRC}_n$. Using the same notations as above, one can mathematically express MAD between $\overline{AECRS1.0}_{10yr}$ and $\overline{CCVRC}_n$ as:

$$MAD^N(AECRS1.\ 0_{10yr}, \overline{CCVRC}_n) = \frac{1}{N} \sum_{i=1}^{N} |(AECRS1.\ 0_{10yr}(i) - \overline{CCVRC}_n)| \quad (2)$$

In equations (1) and (2), $\overline{CCVRC}_n = (\frac{1}{N} \times \sum_{i=1}^{N} CCVR_n(i))$ for nth calculator among 10 CCVRCs and $\overline{AECRS1.0}_{10yr} = (\frac{1}{N} \times \sum_{i=1}^{N} AECRS1.\ 0_{10yr}(i))$. All the calculators were then ranked in an ascending order of the mean deviations.

4.6. Metric 7: ranking of ten CCVR calculators based on kappa coefficients

Since AECRS1.0_{10yr} and the ten CCVRCs measure the CV risk for the same patient, Cohen's Kappa coefficients is a good choice to test the agreement between AECRS1.0_{10yr} and the ten CCVRCs. AECRS1.0_{10yr} and the ten CCVRCs were converted into binary class labels for each patient (i.e., high-risk and low-risk class). SPSS was used to compute the Kappa coefficients and the significance level. The calculator with highest Kappa value indicates the highest agreement and closeness with AECRS1.0_{10yr}. All the ten CCVRCs were then ranked in descending order to investigate the closeness between the CCVRCs and AECRS1.0_{10yr} results.

4.7. Metric 8: logistic regression and ROC analysis for ranking the CCVRCs

Multivariate logistic regression (MLR) was performed to determine the best CCVR calculator that can predict the high-risk class patients. The performance of the ten CCVRCs was evaluated using odds ratios (OR). Odds ratios were adjusted using significant confounding factors such as fasting blood sugar (FBS), SBP, and DBP derived using *t*-test on baseline characteristics. The probabilities obtained from MLR for each of the ten CCVRCs were used to perform the ROC analysis. ROC analysis is a fundamental tool to test the performance of two calculators with reference to the gold standard. It is a curve of true positive rate plotted against false positive rate for varying CV risk threshold points. Any point on the ROC curve provides the sensitivity and specificity of the two CV risk calculators. AUC value tells how much accurately the high-risk patients can be identified using the two calculators under consideration. In order to avoid any bias in the ranking process, the gold standard was derived from the combination of both image-based

phenotypes (i.e., IMT_{max} and PS) and CCVR factors (i.e., HT and HbA1c). Thus the gold standard risk classification variable used for MLR and ROC analysis was obtained from the combination of four risk factors (IMT_{max}, HbA1c, HT, and PS). This combination of classification variables was then used to minimize the effect of larger magnitudes of OR.

4.8. Cumulative ranking-based score for all the CCVR calculators

A cumulative ranking score was developed, which is an average value of the ranking of all the ten CCVR calculators over eight metrics. The overall cumulative ranking-based score provides the final ranking of the ten CCVRCs which decides the performance of the $AECRS1.0_{10yr}$ with each of the ten CCVRCs. The cumulative ranking provides the full coverage of the overall ranking of the CCVRCs with respect to $AECRS1.0_{10yr}$.

5. Results

5.1. Baseline evaluation

Table 1 indicates the baseline characteristics for the Japanese Population recruited in the current study. The pool of 202 patients had a mean age of 68.97 ± 10.96 years, ranging from 29 years to 88 years. The Japanese cohort in the current study had 50% of patients which were less than 70 years old and about 33% of patients were less than 55 years. Further, 20% of this cohort (less than 70 years old) had high diabetes (≥6.5%). Second, 50% of the cohort (that is less than 70 years old) also had high hypertension (> 140–200 mm Hg). About 10% of the cohort (that is less than 70 years old) had a family history of coronary artery disease. The conventional factors like diabetes, hypertension, and family history were affecting 50% of the cohort. This means they were most likely to be in the very high-risk pool if not checked or monitored regularly. This indicates that these patients were less likely to reach a life expectancy of 83.2 years of Japan [58], if not carefully monitored. This clearly shows that this cohort can benefit from the 10-year risk prediction tool when tried upon. Table 1 also indicates the baseline characteristics of the patients which were risk-stratified into the high-risk or low-risk class using a classification variable (Gold standard) which was a combination of four risk factors such as glycated hemoglobin (HbA1c), hypertension (HT), plaque score (PS), and maximum IMT (IMT_{max}). From Table 1, it has been observed that HbA1c, systolic blood pressure, diastolic blood pressure, plaque score, and hypertension were the confounding factors with a significance level of < 0.05. A summary of the abbreviations of the CV risk factors is shown in Appendix-Table 2.

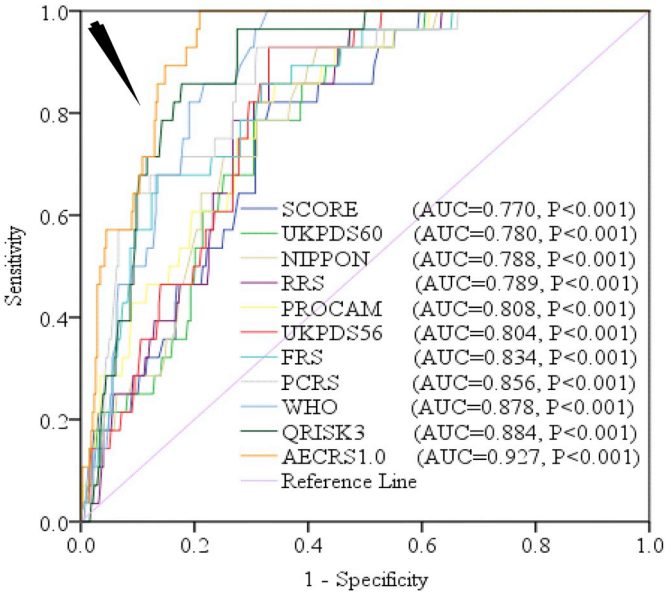

Fig. 2. Ranking of eleven cardiovascular calculators using ROC analysis. The black arrow indicates the ROC plot for the $AECRS1.0_{10yr}$ which shows the highest area-under-the-curve (AUC). The calculators are arranged as per increasing AUC's. Shown are also the corresponding p values.

5.2. Ranking based on similarity index

Each of the ten CCVRCs was ranked in a descending order of their similarity index and shown in Fig. 3. QRISK3 indicated the highest similarity to $AECRS1.0_{10yr}$ (Appendix-Table 7, R1) in classifying the patients into the high-risk class (SI = 161.18 ± 15.71) followed by the NIPPON (SI = 141.18 ± 34.89) and the RRS (SI = 138.09 ± 13.28). WHO/ISH risk charts reported the least similarity to $AECRS1.0_{10yr}$ while classifying the patients into the high-risk class (SI = 6.09 ± 0.30). The variation in similarity index was possibly because of the number of CCVR factors for which the particular risk calculator was originally developed (Appendix-Table 5). QRISK3 was developed for 22

Table 1
Baseline characteristics of the patients divided into low-risk and high-risk classes.

SN	C1	C2	C3	C4	C5
R1	Parameters	Overall	High-Risk	Low-Risk	P-Value
R2	Total (n)	202	18	184	–
R3	Male, n (%)	156 (77.23%)	13 (8.33%)	143 (91.67%)	0.578
R4	Female, n (%)	46 (22.77%)	5 (10.87%)	41 (89.13%)	0.578
R5	Age (years)	68.97 ± 10.96	69.33 ± 8.87	68.93 ± 11.16	0.233
R6	Smoking, n (%)	81 (40.10%)	8 (9.88%)	73 (90.12%)	0.995
R7	HbA1c (%)[a]	6.28 ± 1.11	7.59 ± 1.03	6.15 ± 1.03	0.001
R8	FBS (mg/dl)[a]	121.21 ± 34.81	137.78 ± 38.80	119.59 ± 34.08	0.018
R9	LDL-C (mg/dl)	100.75 ± 31.48	101.17 ± 33.16	100.71 ± 31.41	0.996
R10	HT, n (%)[a]	147 (72.77%)	18 (12.24%)	129 (87.76%)	0.048
R11	FH, n (%)	24 (11.88%)	2 (8.33%)	22 (91.67%)	0.418
R12	PS[a]	9.09 ± 5.31	11.72 ± 4.04	8.84 ± 5.36	0.001
R13	HDL-C (mg/dl)	50.49 ± 14.97	49.67 ± 14.04	50.57 ± 15.09	0.951
R14	TC (mg/dl)	174.33 ± 36.73	175.44 ± 33.52	174.22 ± 37.11	0.662
R15	TC/HDL-C	3.65 ± 1.01	3.77 ± 1.18	3.64 ± 1.00	0.671
R16	SBP (mm Hg)[a]	134.55 ± 8.92	140.00 ± 0.00	134.02 ± 9.18	0.048
R17	DBP (mm Hg)[a]	87.28 ± 4.46	90.00 ± 0.00	87.01 ± 4.59	0.048

HbA1c: Glycated Hemoglobin; LDL-C: Low-Density Lipoprotein Cholesterol; HDL-C: High-Density Lipoprotein Cholesterol; TC: Total Cholesterol; SBP: Systolic Blood Pressure; DBP: Diastolic Blood Pressure; FH: Family History; PS: Plaque Score.
[a] Significant Cofounding factors.

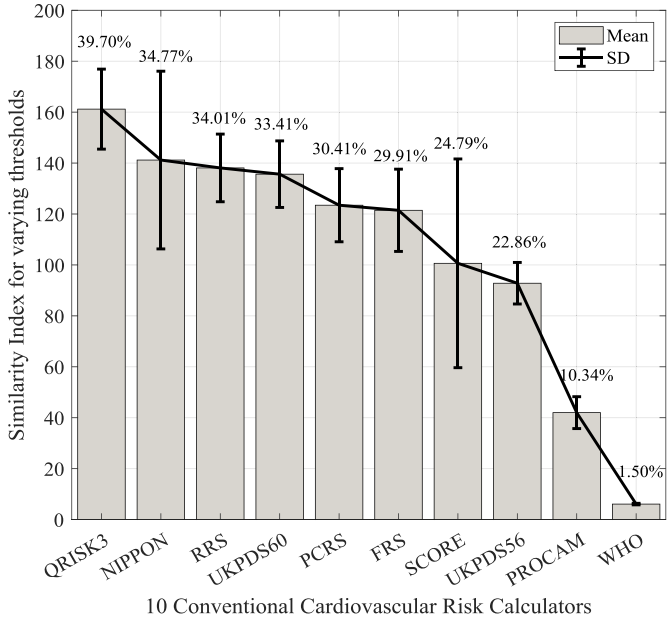

Fig. 3. Ranking of similarity index (Metric Type-M1) between AECRS1.0_{10yr} and ten CCVR calculators.

CCVR factors. QRISK3 also reported the least variation in terms of individual metric ranking when analyzed using eight different metrics (Table 2 Row 1, M1 to M8).

5.3. Clustering-based ranking

Adapting the clustering-based ranking algorithm for a CCVRC, one can compute the closeness of the CCVRC against AECRS1.0_{10yr}. Fig. 4 (A-D) shows the closeness of the ten CCVRCs (RC1 to RC10) against AECRS1.0_{10yr} for four types CCVR factors. The CoM for the UKPDS60 calculator was consistently closer to the CoM of the AECRS1.0_{10yr}. In Fig. 4 (A) and Fig. 4 (C), it appears that RC1 i.e., FRS is closer to the AECRS1.0_{10yr} compared to UKPDS60. This is mainly because of the unequal and elongated grid resolution (1:20, 1:10, 1:20, and 1:100 units for Fig. 4 (A-D), respectively). Appendix-Table 8 shows the minimum Euclidean distances between AECRS1.0_{10yr} and UKPDS60 as 5.36, 4.74, 5.52, and 5.42 units, for the clusters corresponding to risk covariates age, TC, SBP, and HbA1c, respectively (columns: C3, C4, C5, and C6, respectively). Ranking of all the ten CCVRCs was calculated for the four clusters corresponding to four risk factors (i.e., age, TC, SBP, and HbA1c). Appendix-Table 8 shows the ranking for the ten CCVRCs based on the clustering method. Note that the top three calculators remained consistent for all the four risk factors (column C3-C6).

5.4. Ranking using PoM and FoM

In PoM, normalized mean absolute difference between $CCVRC_n$ and AECRS1. 0_{10yr} was computed, while in FoM, the normalized mean absolute difference between $\overline{AECRS1.0}_{10yr}$ and $\overline{CCVRCn}$ was computed. Appendix-Table 9 (column C4 and C6) shows the ranking of the ten CCVRCs using the metrics "PoM and FoM". Using PoM, the top three calculators were: FRS, QRISK3, and UKPDS60 (see column C3). Using FoM, the top three calculators were UKPS60, FRS, and QRISK4 (see column C5). FRS ranked first with a PoM and FoM of 53.66% and 81.98%, respectively (see row R1, column C9, and column C11, respectively). UKPDS60 ranked first among the ten CCVRCs with a PoM and FoM 39.30% and 95.13%, respectively. These were quite consistent with the other metrics.

5.5. Ranking based on mean deviation

Using the mathematical representation of equations (1) and (2), we compute the deviation of $CCVRC_n$ from $\overline{AECRS1.0}_{10yr}$ and deviation of AECRS1.0_{10yr} from $\overline{CCVRC}_n$. This can be seen in Appendix-Table 10. Column C3 shows the deviation of $CCVRC_n$ from $\overline{AECRS1.0}_{10yr}$ while C5 shows the deviation of AECRS1.0_{10yr} from $\overline{CCVRC}_n$. The corresponding ranking for all the calculators is shown in Fig. 5 (also in column C6 of the Appendix-Table 10). Fig. 5 shows that the top three calculators are FRS, QRISK3, and UKPDS60 in both of the deviation methods (which are indicated by black arrows), however their ranking slightly interchanges while contesting for the first three positions. Also, it is to be noted that the deviation of $CCVRC_n$ from $\overline{AECRS1.0}_{10yr}$ is slightly higher compared to the deviation of AECRS1.0_{10yr} from $\overline{CCVRC}_n$. This does not affect the ranking since the calculators are relatively positioned.

5.6. Ranking based on kappa coefficients

Using the strategy discussed in the methodology section, we convert AECRS1.0_{10yr} and ten $CCVR_n$ into a binary class labels for each patient (i.e., the high-risk and low-risk class). This data was fed to SPSS to compute the Kappa coefficients. Column C9 in Table 2 demonstrates the ranking of ten CCVRCs using Kappa coefficients. The observations show that the top three calculators as per the Kappa coefficients are RRS, QRISK3, and SCORE. QRISK3 maintained its leadership in the top three positions. The effectiveness of kappa is not strong due to the lack of covariates (risk factors) in the SCORE calculator (Appendix-Table 5).

5.7. Ranking based on LR, Odd's ratio and area-under-curve

Performance of all CV risk calculators (ten CCVR calculators and the integrated risk calculator AECRS1.0_{10yr}) was evaluated using ROC analysis (Fig. 2). Furthermore, all the 11 risk CV calculators were

Table 2
Cumulative ranking of the 10 CCVR calculators based on eight performance evaluation metrics.

C1	C2	C3	C4	C5	C6	C7	C8	C9	C10	C11
#SN	Calculator	Similarity Measure (M1)	Cluster Measure (M2)	PoM (M3)	FoM (M4)	Deviation from mean AECRS1.0 (M5)	Deviation from mean CCVRC (M6)	Kappa Coefficient (M7)	LR (M8)	Cumulative Ranking
R1	QRISK3	1	3	2	3	2	3	2	1	2.1
R2	FRS	6	2	1	2	1	2	6	4	3.0
R3	UKPDS60	4	1	3	1	3	1	8	9	3.8
R4	RRS	3	5	4	5	5	5	1	7	4.4
R5	UKPDS56	8	4	5	4	4	4	7	6	5.3
R6	NIPPON	2	6	6	6	6	6	9	8	6.1
R7	PROCAM	9	7	7	7	7	7	5	5	6.8
R8	PCRS	5	9	9	9	9	9	4	3	7.1
R9	WHO	10	8	8	8	8	8	10	2	7.8
R10	SCORE	7	10	10	10	10	10	3	10	8.8

LR: Logistic Regression; PoM: Precision-of-Merit; FoM: Figure-of-Merit.

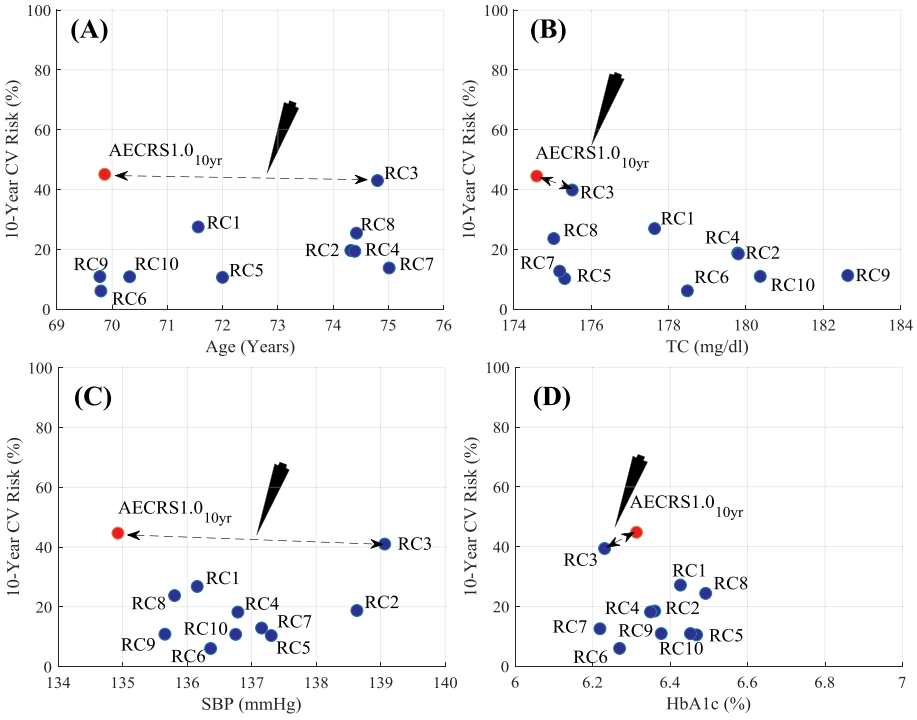

Fig. 4. Ranking based on clustering method (Metric Type-M2)to investigate the closeness between AECRS1.0$_{10yr}$ and ten CCVR calculators. Black arrows indicate the minimum Euclidean distance between the center-of-mass values of AECRS1.0$_{10yr}$ and one of the ten CCVR calculators. RC1:FRS; RC2:UKPDS56; RC3:UKPDS60; RC4:RRS; RC5:PCRS; RC6:SCORE; RC7:NIPPON; RC8:QRISK3; RC9:PROCAM; RC10:WHO/ISH charts. The grid resolution for the plots in Fig. 4 (A–D) is 1:20, 1:10, 1:20, and 1:100 units, respectively.

ranked in an ascending order of AUC (Appendix-Table 11) values such as: (i) AECRS1.0$_{10yr}$ (AUC = 0.927, P < 0.001), (ii) QRISK3 (AUC = 0.884, P < 0.001), (iii) WHO chart (AUC = 0.878, P < 0.001), (iv) PCRS (AUC = 0.856, P < 0.001), (v) FRS (AUC = 0.834, P < 0.001), (vi) PROCAM (AUC = 0.808, P < 0.001), (vii) UKPDS56 (AUC = 0.804, P < 0.001), (viii) RRS (AUC = 0.789, P < 0.001), (ix) NIPPON (AUC = 0.788, P < 0.001), (x) UKPDS60 (AUC = 0.780, P < 0.001), and (xi) SCORE (AUC = 0.770, P < 0.001). AECRS1.0$_{10yr}$ reported the highest AUC compared to all other CCVRCs. Appendix-Table 11 shows the ranking of the calculators using AUC, where it shows AECRS1.0$_{10yr}$ as the first rank followed by QRISK3 (column C9). Note that SCORE is the lowest rank in the list of all calculators.

5.8. Cumulative ranking-based score

All the ten CCVRCs were compared against AECRS1.0$_{10yr}$ using eight performance metrics. Table 2 shows the performance metrics ranked the ten CCVRCs on the scale of 1–10. A cumulative ranking-based score was then computed by taking an average of all eight ranks computed from the eight different metrics, as shown in column C11. The order of the metrics from M1 to M8 was: similarity measure, cluster measure, PoM, FoM, deviation from the mean of AECRS1.0$_{10yr}$, deviation from the mean CCVRC, kappa coefficient, and logistic regression. As seen from Table 2, QRISK3 ranked at the first place with a cumulative ranking-based score of 2.1 (row R1 and column C11) whereas, SCORE-based calculator ranked at the 10th place with the cumulative rank of 8.8 (row R10 and column C11). Thus, the proposed AECRS1.0$_{10yr}$ was closest to the well-known, popular, and most effective risk calculator QRISK3. Logistic regression and similarity index showed that the QRISK3 calculator has consistently the highest feature retaining power, as shown by its loweset final cumulative risk score. FRS and UKPDS60 ranked at second and third places, respectively. FRS performed well, primarily due to a larger age group in the cohort.

6. Discussion

6.1. Summary and hypothesis

A comparative study of 11 CV risk calculators including ten CCVRCs (FRS, UKPDS56, UKPDS60, RRS, QRISK3, PCRS, SCORE, NIPPON, PROCAM, and WHO) and one “image-based phenotype fused with CCVR factors”, so-called “integrated risk calculator” (named as: AECRS1.0$_{10yr}$) was presented to perform a risk stratification of a diabetic Japanese cohort. Eight different statistical metrics (M1-M8) were designed to evaluate the performance of AECRS1.0$_{10yr}$ by comparing against the ten CCVRCs. Each performance metric was then adapted to rank the ten conventional CV risk calculators. Finally, all the ranking scores using our eight metrics were accumulated to derive the cumulative ranking score that decided the ranking of the ten CCVRCs when comparing their closeness to AECRS1.0$_{10yr}$. Our study proved the two major hypotheses. AECRS1.0$_{10yr}$ computes the 10-year atherosclerotic plaque measurements using current plaque measurements along with the CCVR factors transformed into the image domain as projection rates. Because this calculator has a direct impact on atherosclerosis disease, and also shows the highest AUC (Fig. 2, AUC = **0.927**, P < 0.001), our first hypothesis is proved. The second important point to observe is that since QRISK3 had the highest number of covariates in its design and uses Cox regression model for which comes from a very large cohort, it picks the high-risk patients very well and hence achieves the highest ranking. As a result, this is the closest calculator to AECRS1.0$_{10yr}$ and proves the second hypothesis. A deeper analysis of the performance of the architecture will be discussed after the benchmarking of risk calculators.

6.2. Benchmarking of the risk calculators

Table 3 shows the benchmarking table which compares several studies presented in chronological order taken from 2009 to 2017 (row R1 to row R10). The table has six columns (C2 to C7) corresponding to the attributes: authors/year, type of the calculators used in the study, total patients in the study, the threshold used by the calculators to

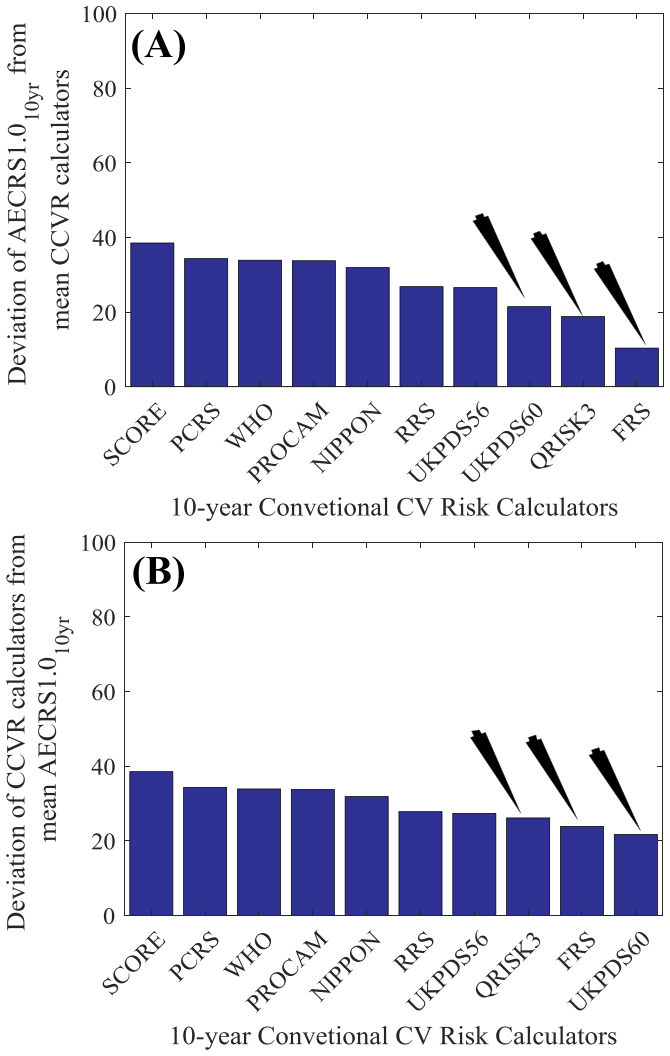

Fig. 5. Ranking of the ten conventional cardiovascular risk calculators using deviation method. (A) Ranking based on deviation from mean AECRS1.0$_{10yr}$ (Metric Type-M5). (B) Ranking based on the deviation of mean CCVR calculators (Metric Type-M6). Black arrows indicate the conventional cardiovascular risk calculators with least mean deviation from AECRS1.0$_{10yr}$. Also except the CCVR calculators indicated by black arrows, positions of all the CCVR calculators remains the same.

determine the risk, CCVRC vs. integrated calculator, and the performance metrics adapted in their studies. To begin with, column C6 shows the striking difference between all studies (row R1 to row R10) against the proposed study (row R11) in terms of the calculator architecture (shown as a cross in all studies R1 to R10 vs. acceptance tick for proposed study). This fundamental difference is the key novelty of the study named after the composite risk score using AtheroEdge (so-called AECRS1.0). This means, the proposed study used imaging-based phenotypes combined with CCVRC as a 10-risk prediction model.

The second most striking observation is that all previous studies (row R1 to R10) used up to a maximum of six risk calculators in their comparative work, while the proposed study used 11 risk calculators (AECRS1.0$_{10yr}$, FRS, UKPDS56, UKPDS60, RRS, PCRS, QRISK3, SCORE, NIPPON, WHO, PROCAM). This study offered an added advantage to the diversity of the origin of calculators, by diversity we mean, which countries participated in the calculator design, such as Australia (row R1) [59], Korea (row R2) [60], USA (row R3) [61], England (row 4,6,8, and 9) [62–65], and India (row 7 and 10) [66,67]. Another very important observation is that all the studies adapted one or at the most three metrics for evaluation of their calculators (column C7). On the contrary, the proposed study adapted eight different metrics (row R11 and column C7) such as: M1: similarity index, M2: clustering, M3: precision-of-merit, M4: figure-of-merit, M5: deviation from mean AECRS1.0$_{10yr}$, M6: deviation of AECRS1.0$_{10yr}$ from mean CCVRC, M7: kappa coefficient, M8: logistic regression and ROC analysis (Appendix-Table 3). This was the key contribution and innovation in our study primarily used for the evaluation of AECRS1.0$_{10yr}$. Lastly, we wanted to point out that most of the previous studies used FRS and QRISK2 or QRISK3 in their comparative studies. However, in the proposed study, a total of 11 different CV risk calculators are presented for comparison, therefore we can be confident in the performance of AECRS1.0$_{10yr}$ against a greater majority of CCVRCs. In our proposed study, QRISK3 showed the best performance with the topmost ranking (having the least ranking score), which is also well adapted clinically ([11,65,66]). In comparison to QRISK3, AECRS1.0$_{10yr}$ showed a higher AUC, in addition to being fully automated. Further, AECRS1.0$_{10yr}$ was derived from AtheroEdge2.0 which was validated against CT and physician's gold standards [52,53]. Thus this clearly demonstrates that AECRS1.0$_{10yr}$ not only can be adapted clinically but also has comparable or better performance compared to QRISK3. We will examine the column C5, the thresholds used for the risk stratification, in the next subsection.

6.3. Thresholds for risk stratification between different calculators

It has been observed that the performance of CCVRCs varies with risk stratification thresholds. In this study we have tested two types of thresholds: (i) international thresholds and (ii) proposed thresholds (Appendix-Table 12). As the name suggests, the difference lies in the way the threshold was adapted: thresholds taken from previous studies vs. the threshold of the proposed study. International thresholds are the ones which were recommended or used in the cohort studies or clinical trials [63,64,66–69]. Multiple studies have been reported in the literature to stratify the patients into the high-risk class using a specific threshold which varies among the calculators. These risk thresholds also decide the statin eligibility of the patients while classifying them into a high-risk category. Garg et al. [66] used a 20% threshold for FRS, QRISK2, PCRS (or ASCVD) and WHO calculators to classify the patients into the high-risk class. Selvarajah et al. [68] adopted a 20% risk threshold for FRS and a 30% threshold for the WHO risk calculator. Bosomworth et al. [69] defined the high-risk class for the patients if RRS as more than 20%. Dalton et al. [64] used a threshold of 20% for risk stratification using QRISK2. Santos et al. [63] presented a comparative study of the SCORE and PCRS calculators with risk-thresholds of 5% and 7.5%, respectively. A similar comparative study between the FRS and UKPDS calculators for the Indian population was presented by Bansal et al. [67] which used a common threshold of 20% for both risk calculators. From these studies, it has been clear that the risk thresholds are calculator-specific and can be different for different cohorts.

There were three calculators marked with "*" where previous studies have provided a range of threshold values. RRS calculator showed a range from 10% to 20% [12,70], NIPPON showed the risk between 5% and 10% [13], and QRISK3 showed the range from 10% to 20% [11,71]. The column C3 (Appendix-Table 12) showed the difference between the international and proposed thresholds. In our proposed study, we took the lower cutoff for international calculators which had the range of variation (column C3) and our proposed threshold were similar to the international threshold for FRS, UKPDS56, UKPDS60, PCRS, SCORE, WHO, and PROCAM calculators. From our experience, we noticed that the baseline high-risk nature of the population may have an additional impact while selecting the risk-thresholds. The Japanese cohort under consideration had elevated risk profile at baseline with an average cIMT value of 0.95 mm. Therefore slightly different thresholds were used for QRISK3, NIPPON, and RRS calculators which were also in line with the previous studies published studies [13,62,70,71]. Except for the NIPPON, PROCAM, PCRS, WHO and

Table 3
Benchmarking of the current study with previously published comparative analysis studies for the risk calculators.

C1	C2	C3	C4	C5	C6	C7
#SN	Author (Year)	Calculator Types	Total Patients	Thresholds for Calculators	Imaging Phenotypes Used?	Performance Metric
R1	Davis et al. [59] (2009)	FRS, UKPDS	815	10%	✗	AUC
R2	Ahn et al. [60] (2011)	FRS, UKPDS, SCORE	1275	–	✓	AUC, OR
R3	Cook et al. [61] (2012)	ATP III, FRS, RRS	3716	10%	✗	c-Statistics, NRI, IDI
R4	Simmonds et al. [62] (2012)	FRS (1991), FRS (2008), RRS, ASSIGN, QRISK2, SCORE	500000	FRS-1991(15%), FRS-2008(18%), ASSIGN (21%), RRS (11%), SCORE (4%), QRISK2 (16%)	✗	Sensitivity, Specificity, Accuracy
R5	Selvarajah et al. [68] (2014)	FRS, SCORE, and WHO/ISH	14863	FRS (> 20%), SCORE (> 5%), and WHO (> 30%)	✗	ROC
R6	Santos et al. [63] (2015)	SCORE and ASCVD	446	7.5% for ASCVD and 5% for SCORE	✗	ROC, H-L Test
R7	Bansal et al. [67] (2015)	FRS and UKPDS	489	20% for both	✗	Kappa Statistics
R8	Dalton et al. [64] (2015)	QRISK2 and JBS2		> 20%	✗	Kappa Statistics
R9	Alemao et al. [65]. (2017)	FRS and QRISK2	4780	–	✗	AUC, AIC, NRI
R10	Garg et al. [66] (2017)	FRS, QRISK2, JBS3, ASCVD, WHO charts	1110	20%	✗	Wilcoxon Signed Ranked Test and Mc-Nemar Test
R11	Proposed (2018)	AECRS1.0$_{10yr}$, FRS, UKPDS56, UKPDS60, RRS, PCRS, QRISK3, SCORE, NIPPON, WHO, PROCAM	202	45%	✓	[a]M1, M2, M3, M4, M5, M6, M7, M8

FRS: Framingham Risk Score; UKPDS: United Kingdom Prospective Diabetes Study; RRS: Reynolds Risk Score; SCORE: Systematic coronary risk evaluation; PCRS: Pooled Cohort Risk Score; ROC: Receiver Operating Characteristics; AIC: Akaike Information Criterion; NRI: Net Reclassification Index; OR: Odds Ratio.

[a] M1: Deviation from mean AECRS1.0$_{10yr}$, M2: Deviation of AECRS1.0$_{10yr}$ from mean CCVRC, M3: Logistic Regression, M4: Similarity Index, M5: Clustering, M6: Precision-of-Merit, M7: Figure-of-Merit, M8: Kappa coefficient.

SCORE calculators which were ranked in the bottom of the cumulative ranking table, all other calculators' ranking position varied by using the proposed or international threshold scheme.

6.4. Justification of risk threshold for AECRS1.0_{10yr}

In our proposed study using AECRS1.0_{10yr}, a risk threshold of 45% was used to risk-stratify Japanese patients. The comparative effect of this was the same as the CCVRCs, except that AECRS1.0_{10yr} had higher dynamic ranges of the classes. By dynamic range of classes, we mean the difference between the upper cutoff and the lower cutoff values of the risk class. Due to this larger dynamic range, the class range has stretched. Further, to begin with, we had six classes in AECRS1.0_{10yr}, and this caused the class range to have bigger values. As a result, the class threshold was apparently higher compared to CCVRCs. The key advantage of having six classes was to have a better risk stratification and control on the manifestation of the risk. The risk thresholds used for the initiation of statins are generally dependent upon the risk prediction model, baseline characteristics of the patients, and the risk factors included in the risk calculator. Since AECRS1.0_{10yr} is an integrated CV risk calculator that combines both the CCVR factors and image-based phenotypes, the risk thresholds used for other CCVRCs may not be applicable for AECRS1.0_{10yr} and vice-versa. Furthermore, the Japanese cohort used in this study indicated a moderate to high-risk profile at baseline. Thus, our threshold of 45% was consistent with the baseline characteristics. Using the proposed threshold of 45%, AECRS1.0_{10yr} stratified 44.58% of overall ultrasound scans into the high-risk class. The similarity index of QRISK3 reported the highest closeness with AECRS1.0_{10yr} with 39.70% of the overall scans with a high-risk status (Fig. 3). The Japanese ethnicity-based CCVRC called NIPPON was at second place with 34.77% of the population in high-risk class (Fig. 3). The total number of high-risk ultrasound scans identified by AECRS1.0_{10yr} was within the range of ± 5% of the QRISK3 which was also ranked at first place by the cumulative ranking score. This clearly validates the corresponding threshold used for AECRS1.$0_{10yr.}$

6.5. Ranking of conventional cardiovascular risk calculators

Closeness between AECRS1.0_{10yr} and the ten CCVRCs was evaluated using a cumulative ranking score. QRISK3 and FRS were ranked in the top two positions, respectively, followed by UKPDS60 and UKPDS56. QRISK3 has ranked in top two places compared to other calculators in pretty much all performance metrics. One plausible justification is the number of risk factors in their design of the risk prediction model. QRISK3 was designed for the highest number of CCVR factors (i.e., 22 risk factors). Furthermore, QRISK3 showed a similarity measure of nearly 40% (Appendix-Table 7) when compared to AECRS1.0_{10yr} for risk stratification of high-risk patients. In the current study, chart-based risk calculators such as WHO, SCORE, NIPPON, and PROCAM were ranked lower compared to the QRISK3. Out of eight performance metrics, six metrics ranked SCORE calculator in the last position. In this diabetic cohort, HbA1c is an important risk factor. 10-year risk prediction models such as UKPDS60, NIPPON, and SCORE did not have HbA1c as an independent risk factor in their risk prediction model (Appendix-Table 5). This may be another important reason for these calculators to be ranked in an intermediate to lower positions in the cumulative ranking table.

6.6. A note on statistical metrics for studying the closeness between AECRS1.0_{10yr} and CCVRCs

Among the eight statistically derived metrics were used to evaluate the performance of AECRS1.0_{10yr} with ten conventional calculators. The primary objective of these eight performance evaluation metric is to identify the closest CCVRC to that of AECRS1.0_{10yr}. The similarity index metric (metric M1) was important to identify the patients who were stratified into high-risk category by both of the AECRS1.0_{10yr} and CCVR calculator under consideration. Based on this similar high-risk patient identification criterion, similarity index based ranking has indicated the highest closeness between AECRS1.0_{10yr} and QRISK3. Among eight statistical metrics, logistic regression and similarity index were the most computationally expensive but had an influential impact on the cumulative ranking score. Both of these metrics have ranked QRISK3 at the first place indicating that they are closer to AECRS1.0_{10yr} (Table 2, row 1, column C3 and C10). FoM and deviation of AECRS1.0_{10yr} from the mean CCVRCs showed consistent ranking for all the ten CCVR calculators (Table 1). PoM and deviation of ten CCVRCs from the mean AECRS1.0_{10yr} showed consistent ranking for QRISK3, FRS, and UKPDS60 (Table 2).

6.7. A note on sensitivity analysis of eleven calculators' coefficients

In this study, the performance of AECRS1.0_{10yr} was evaluated against ten CCVRCs. Computation of 10-year risk using CCVRCs such as WHO, PROCAM [17], SCORE [14], and NIPPON [13] was based on the predefined standard risk charts. Remaining seven CCVRCs such as FRS [8], UKPDS56 [9], UKPDS60 [10], RRS [12], PCRS [16], and QRISK3 [11] were derived using a predefined set of coefficients which were obtained using Cox regression analysis. In this study, all the CCVRCs were used in original settings without altering their predefined coefficients. However, the coefficients from all these CCVR calculators were varied by 0.1%–2% to investigate the sensitivity analysis of these calculators. It has been observed that the net effect on the 10-year risk computed using all CCVRCs varied only by ± 5%. Due to this low sensitivity, all the ten CCVRCs were used in their original form.

6.8. A special note of sample size

In general, data sample is defined as "a set of data collected or selected from the statistical population by a defined procedure" [72]. The defining procedure only ensures that the samples must not be repeated, i.e., it must not be the identical. In this study, we followed this standardized protocol for the data sample collection [73–75]. The same concept of data sample collection was adapted for collecting multiple samples from the same body but not identical samples. Although the two carotid arteries (i.e., the left CCA and right CCA) have similar genetic makeup and functionality of supplying the oxygenated blood to the brain, but the arteries worked independently along the different pathways. Note that the shape of the artery, bifurcation of the artery from the aorta follows different paths (via innominate artery vs. via aortic artery) [76,77]. Furthermore, atherosclerotic plaque is multifocal in nature and follows an independent deposition of the disease along the two artery types [77,78]. Thus, the samples of the left CCA and right CCA has no similarity in shape, size, structure, composition, physics of the formation of atherosclerotic plaque, and pathways leading to brain. As a result, each of the 404 ultrasound scans collected from the left and right CCA can be considered as an independent sample during power analysis.

6.9. Effect of bias on performance evaluation

It is to be noted that all the ten CCVRCs were independently designed for different ethnic population, and to compare them, one must therefore keep the same input source of cohort. Here, the Japanese cohort was taken to evaluate all the ten CCVRCs for comparing against AECRS1.$0_{10yr.}$ Thus, there is no bias due to Japanese cohort itself.

Another type of bias can be due to the gold standard (so-called as the response variable). The gold standard used in this study for ROC and MLR analysis was derived using the combination of the image-based phenotypes (i.e., IMT_{max} and PS) and conventional cardiovascular risk factors (i.e., hypertension, symbolized as HT and hemoglobin A1c, symbolized as HbA1c). Thus, the gold standard response variable for the risk classification using MLR and ROC analysis was obtained

using the combination of four risk factors (IMT_{max}, HbA1c, HT, and PS). The main idea behind selecting a diverse combination of covariates for response variable was to ensure no bias while computing the performance of risk calculators.

6.10. Strengths, limitations, and future extensions

This is the first study of its kind that compared 11 cardiovascular risk calculators using data from a Japanese diabetic cohort. Furthermore, this study has evaluated the performance of the carotid ultrasound image-based phenotype risk calculators called $AECRS1.0_{10yr}$ against the ten CCVRCs using eight statistical metrics. In spite of the strengths, there are some limitations: (i) even though, our power analysis showed enough cohort size, this study mainly focused on a Japanese cohort with relatively smaller sample size and (ii) clinical endpoints such as CVD mortality rates were not included in this study due to their non-availability. Although the ROC analysis presented in this study ranked $AECRS1.0_{10yr}$ at the first place, we believe that more longitudinal trials need to be performed with clinically relevant endpoints to validate the performance of $AECRS1.0_{10yr}$ in different ethnicity cohorts.

7. Conclusion

We presented an integrated risk calculator called "AtheroEdge Composite Risk Score ($AECRS1.0_{10yr}$)" that was recently developed and computes the 10-year risk of carotid image phenotypes by integrating conventional cardiovascular risk factors (CCVRFs). We study the closeness between $AECRS1.0_{10yr}$ against the ten other currently available conventional cardiovascular risk calculators (CCVRCs): QRISK3, Framingham Risk Score (FRS), United Kingdom Prospective Diabetes Study (UKPDS) 56, UKPDS60, Reynolds Risk Score (RRS), Pooled cohort Risk Score (PCRS or ASCVD), Systematic Coronary Risk Evaluation (SCORE), Prospective Cardiovascular Munster Study (PROCAM) calculator, NIPPON, and World Health Organization (WHO) risk. The cumulative ranking was computed using eight different statistically derived metrics. $AECRS1.0_{10yr}$ reported the highest area-under-the-curve (**0.927**;$P < 0.001$) among all the risk calculators. Top three CCVRCs, the closest to $AECRS1.0_{10yr}$ were: QRISK3, FRS, and UKPDS60. $AECRS1.0_{10yr}$ demonstrated the best performance due to the integration of image-based phenotype with CCVR factors and ranked at first place with the highest AUC. Cumulative ranking of ten CCVRCs demonstrated that QRISK3 was the closest calculator to $AECRS1.0_{10yr}$, which is also consistent with the industry trend.

Conflicts of interest

None.

Financial Support/grants

None.

Disclosure

Dr. Jasjit Suri is affiliated to AtheroPoint™, focused in the area of stroke and cardiovascular imaging.

Acknowledgements

None.

Appendix

Appendix-Table 1
Abbreviation table pertaining to risk calculators and carotid anatomy.

C1	C2	C3
#SN	Abbreviation	Meaning
R1	CCVR	Convectional Cardiovascular Risk
R2	CCVRC	Conventional Cardiovascular Risk Calculator
R3	CCVRCs	Conventional Cardiovascular Risk Calculators
R4	CCVRF	Conventional Cardiovascular Risk Factor
R5	CCVRFs	Conventional Cardiovascular Risk Factors
R6	RC	Risk Calculator
R7	FRS	Framingham Risk Score
R8	UKPDS	United Kingdom Prospective Diabetes Study
R9	RRS	Reynolds Risk Score
R10	PCRS	Pooled cohort Risk Score
R11	ASCVD	Atherosclerosis Cardiovascular Disease
R12	SCORE	Systematic Coronary Risk Evaluation
R13	PROCAM	Prospective Cardiovascular Munster Study
R14	WHO	World Health Organization
R15	AECRS	AtheroEdge Composite Risk Score
R16	CVD	Cardiovascular Diseases
R17	CV	Cardiovascular
R18	CCA	Common Carotid Artery

Appendix-Table 2
Abbreviation table pertaining to cardiovascular risk factors.

C1	C2	C3	C4	C5	C6
#SN	Abbreviation	Description	R15	ED	Erectile Dysfunction
R1	LDL	Low Density Lipoprotein	R16	hsCRP	High Sensitivity C Reactive Protein
R2	HDL	High Density Lipoprotein	R17	cIMT	Carotid Intima Media Thickness
R3	TC	Total Cholesterol	R18	IMTave	Current average value of cIMT

(*continued on next page*)

Appendix-Table 2 (*continued*)

C1	C2	C3	C4	C5	C6
R4	SBP	Systolic Blood Pressure	R19	IMTmax	Current maximum value of cIMT
R5	DBP	Diastolic Blood Pressure	R20	IMTmin	Current minimum value of cIMT
R6	HT	Hypertension	R21	IMTV	Current variability in cIMT
R7	DM	Diabetes Mellitus	R22	TPA	Current carotid plaque area
R8	FH	Family History	R23	$IMTave_{10yr}$	10-year average value of cIMT
R9	HbA1c	Glycated Hemoglobin	R24	$IMTmax_{10yr}$	10-year maximum value of cIMT
R10	TG	Triglyceride	R25	$IMTmin_{10yr}$	10-year minimum value of cIMT
R11	BMI	Body Mass Index	R26	$IMTV_{10yr}$	10-year variability in cIMT
R12	FBS	Fasting Blood Sugar	R27	TPA_{10yr}	10-year carotid plaque area
R13	PS	Plaque Score	R28	mTPA	Morphologic Total Plaque Area
R14	AF	Atrial Fibrillation	–	–	–

Appendix-Table 3
Eight statistical performance evaluation metrics.

C1	C2	C3
#SN	Performance Metrics	Symbolic Representation
R1	Similarity Index	M1
R2	Clustering Method	M2
R3	Precision-of-Merit	M3
R4	Figure-of-Merit	M4
R5	Deviation of CCVR calculators from $\overline{AECRS1.0}_{10yr}$	M5
R6	Deviation of CCVR calculators from $\overline{CCVRC}_n$	M6
R7	Kappa Coefficients	M7
R8	MLR and ROC Analysis	M8

M1 to M8: Metric 1 to Metric 8

Appendix-Table 4
Abbreviation table pertaining to performance metrics.

C1	C2	C3
#SN	Abbreviation	Meaning
R1	SI	Similarity Index
R2	SC	Similarity Count
R3	CoM	Center-of-Mass
R4	CoMs	Center-of-Masses
R5	ED	Euclidean Distance
R6	PoM	Precision-of-Merit
R7	FoM	Figure-of-Merit
R8	MAE	Mean Absolute Error
R9	MAD	Mean Absolute Difference
R10	MLR	Multivariate Logistic Regression
R11	OR	Odds Ratio
R12	ROC	Receiver Operating Characteristics

Appendix-Table 5
. Cardiovascular risk factors used in eleven CV risk calculators.

C1	C2	C3	C4	C5	C6	C7	C8	C9	C10	C11	C12	C13
#SN	Risk Factor	QRISK3	NIPPON	RRS	UKPDS60	PCRS	FRS	SCORE	UKPDS56	PROCAM	WHO	AECRS1.010yr
R1	Ethnicity	✓	–	–	–	✓	–	–	✓		–	✓
R2	Age	✓	✓	✓	✓	✓	✓	✓	✓	✓	✓	✓
R3	Gender	✓	✓		✓	✓	✓	✓	✓		✓	✓
R4	BMI	✓	–	–	–	–	–	–	–	–	–	✓
R5	Smoking	✓	✓	✓	✓	✓	✓	✓	✓	✓	✓	✓
R6	DM	✓	–	✓	–	✓	✓	–	✓	✓	✓	✓
R7	SBP	✓	✓	✓	–	✓	✓	–	–	✓	✓	✓
R8	DBP	–	–	–	–	–	–	–	–	–	–	–
R9	BP Med	✓	–	–	–	–	✓	–	–	–	–	–
R9	LDL	–	–	–	–	–	–	–	–	✓	–	✓
R10	HDL	–	–	✓	–	✓	✓	–	–	✓	–	–

(*continued on next page*)

Appendix-Table 5 (*continued*)

C1	C2	C3	C4	C5	C6	C7	C8	C9	C10	C11	C12	C13
R11	TC	–	✓	✓	–	✓	✓	✓	–	–	✓	✓
R12	TC/HDL	✓	–	–	✓		–	–	–	–	–	–
R13	FH	✓	–	✓	–	–	–	–	✓	✓	–	–
R14	TG	–	–	–	–	–	–	–	–	✓	–	–
R15	CKD	✓	–	–	–	–	–	–	–	–	–	–
R16	Migraine	✓	–	–	–	–	–	–	–	–	–	–
R17	RA	✓	–	–	–	–	–	–	–	–	–	–
R18	SLE	✓	–	–	–	–	–	–	–	–	–	–
R19	SMI	✓	–	–	–	–	–	–	–	–	–	–
R20	ED	✓	–	–	–	–	–	–	–	–	–	–
R21	Steroids	✓	–	–	–	–	–	–	–	–	–	–
R22	AAM	✓	–	–	–	–	–	–	–	–	–	–
R23	AF	✓	–	–	✓	–	–	–	–	–	–	–
R24	hsCRP	–	–	✓	–	–	–	–	–	–	–	–
R25	GT	–	✓		–	–	–	–	–	–	–	–
R26	Artery Type	–	–	–	–	–	–	–	–	–	–	✓
R27	Carotid Phenotypes	–	–	–	–	–	–	–	–	–	–	✓

DM: Diabetes Mellitus; SBP: Systolic Blood Pressure; DBP: Dystonic Blood Pressure; LDL: Low-density Lipoprotein; HDL: High-Density Lipoprotein; TC: Total cholesterol; FH: Family History: TG: Triglyceride: CKD: Chronic Kidney diseases: RA: Rheumatoid Arthritis: SLE: Systemic Lupus Erythematosus; SMI: Sever Mental Illness; BMI: Body Mass Index; ED: Erectile Dysfunction; AAM; Atypical Antipsychotic Medication; AF: Atrial Fibrillation; hsCRP: High Sensitivity C Reactive Protein; GT: Glucose Tolerence

Appendix-Table 6
Symbols pertaining to performance evaluation.

C1	C2	C3
#SN	Symbols	Description
R1	i	Index of the ultrasound image
R2	n	Index of the risk calculator
R3	B	Total number of CCVR Calculators
R4	N	Total number of B-mode ultrasound scans
R5	P	Total number of patients
R6	K	Index of the similarity count
R7	t	Calculator specific global risk threshold
R8	T	Total number of similarity counts
R9	S(t)	Similarity count corresponding to threshold "t"
R10	$\mu_S(CCVRC_n,\ AECRS1.\ 0_{10yr})$	Mean of Similarity counts between $AECRS1.0_{10yr}$ and $CCVRC_n$
R11	$\sigma_s(CCVRC_n, AECRS1.\ 0_{10yr})$	Standard Deviation of Similarity counts between $AECRS1.0_{10yr}$ and $CCVRC_n$
R12	$SI(CCVRC_n, AECRS1.\ 0_{10yr})$	Similarity index between $AECRS1.0_{10yr}$ and $CCVRC_n$
R13	$(x_{CoM}^{AECRS1.0_{10yr}},\ y_{CoM}^{AECRS1.0_{10yr}})$	Center-of-Mass coordinates of $AECRS1.\ 0_{10yr}$
R14	$(x_{CoM}^{CCVRC_n},\ y_{CoM}^{CCVRC_n})$	Center-of-Mass coordinates of $CCVRC_n$
R15	$AECRS1.\ 0_{10yr}(i)$	10-Year CV risk computed using $AECRS1.0_{10yr}$ for ith ultrasound scan
R16	$CCVR_n(i)$	10-Year CV risk computed using nth calculator for ith ultrasound scan
R17	$CCVRC_n$	10-year CV risk computed using nth calculator
R18	$\overline{CCVR}_n$	Average 10-year CV risk computed using nth calculator
R19	$MAD^N(CCVRC_n,\ \overline{AECRS1.0}_{10yr})$	Mean absolute deviation between nth CCVR calculator and average 10-year CV risk computed by $AECRS1.0_{10yr}$
R20	$MAD^N(AECRS1.\ 0_{10yr},\ \overline{CCVRC}_n)$	Mean absolute deviation between $AECRS1.0_{10yr}$ and average 10-year CV risk computed by nth CCVR calculator
R21	$\overline{AECRS1.0}_{10yr}$	Average 10-year CV risk computed using $AECRS1.0_{10yr}$

Appendix-Table 7
Ranking of the ten CCVRCs when compared against AECRS 1.0 using "similarity index" as the metric.

C1	C2	C3	C4	C5	C6
#SN	Calculator Types	Risk Threshold (%)[†]	Similarity Index (Absolute)	Similarity Index (%)	Calculator Rank
R1	QRISK3	10	161.18 ± 15.71	39.70 ± 3.87	1
R2	NIPPON	5	141.18 ± 34.89	34.77 ± 8.59	2
R3	RRS	10	138.09 ± 13.28	34.01 ± 3.27	3
R4	UKPDS60	20	135.64 ± 13.07	33.41 ± 3.22	4
R5	PCRS	7.5	123.45 ± 14.36	30.41 ± 3.54	5
R6	FRS	20	121.45 ± 16.15	29.91 ± 3.98	6
R7	SCORE	5	100.64 ± 40.98	24.79 ± 10.09	7
R8	UKPDS56	20	92.82 ± 8.16	22.86 ± 2.01	8

(*continued on next page*)

Appendix-Table 7 (*continued*)

C1	C2	C3	C4	C5	C6
#SN	Calculator Types	Risk Threshold (%)[‡]	Similarity Index (Absolute)	Similarity Index (%)	Calculator Rank
R9	PROCAM	20	42.00 ± 6.26	10.34 ± 1.54	9
R10	WHO	30	6.09 ± 0.30	1.50 ± 0.07	10

[‡] Proposed thresholds used to stratify the patients into low-risk and high-risk class.

Appendix-Table 8
. Ranking of the ten conventional cardiovascular risk calculators based on the clustering-based metric for all the four conventional risk factors.

C1	C2	C3		C4		C5		C6	
R1	Rank	Risk Factor: Age		Risk Factor: TC		Risk Factor: SBP		Risk Factor: HbA1c	
		Calculator	Distance[†]	Calculator	Distance[†]	Calculator	Distance[†]	Calculator	Distance[†]
R2	1	UKPDS60	5.36066	UKPDS60	4.74792	UKPDS60	5.5261	UKPDS60	5.42201
R3	2	FRS	17.6897	FRS	17.8175	FRS	17.881	FRS	17.6631
R4	3	QRISK3	20.2043	QRISK3	20.9038	QRISK3	20.8972	QRISK3	20.4337
R5	4	UKPDS56	25.8544	UKPDS56	26.2687	UKPDS56	26.1468	UKPDS56	26.3377
R6	5	RRS	26.1298	RRS	26.538	RRS	26.468	RRS	26.638
R7	6	NIPPON	31.7461	NIPPON	31.8069	NIPPON	31.8252	NIPPON	32.2562
R8	7	PROCAM	34.204	WHO	34.0235	PROCAM	33.8074	PROCAM	33.8635
R9	8	WHO	34.2677	PROCAM	34.2014	WHO	33.9055	WHO	33.8804
R10	9	PCRS	34.5232	PCRS	34.2784	PCRS	34.3364	PCRS	34.2995
R11	10	SCORE	39.0292	SCORE	38.5713	SCORE	38.6065	SCORE	38.8171

[†]Euclidean distance between the center-of-mass values of $AECRS1.0_{10yr}$ and CCVR calculators with respect to conventional cardiovascular risk factor as a reference.

Appendix-Table 9
. Ranking of the ten conventional cardiovascular risk calculators using the metric "PoM and FoM".

C1	C2	C3	C4	C5	C6
R1	Rank	Calculator	PoM (%)	Calculator	FoM (%)
R2	1	FRS	53.66	UKPDS60	95.13
R2	2	QRISK3	47.03	FRS	81.98
R3	3	UKPDS60	39.30	QRISK3	79.04
R4	4	RRS	37.72	UKPDS56	73.70
R5	5	UKPDS56	37.26	RRS	73.44
R6	6	NIPPON	29.18	NIPPON	68.15
R7	7	PROCAM	25.01	PROCAM	66.25
R8	8	WHO	24.80	WHO	66.11
R9	9	PCRS	23.34	PCRS	65.68
R10	10	SCORE	13.97	SCORE	61.48

PoM: Precision-of-Merit; FoM: Figure-of-Merit.

Appendix-Table 10
Ranking of the ten conventional cardiovascular risk calculators deviation from mean methods.

C1	C2	C3	C4	C5	C6
#SN	Calculator	$MAD^N(CCVRC_n, \overline{AECRS1.0}_{10yr})^*$	Calculator	$MAD^N(AECRS1.\ 0_{10yr}, \overline{CCVRC}_n)^*$	Calculator Ranking
R1	FRS	21.6949	UKPDS60	10.3529	1
R2	QRISK3	23.8470	FRS	18.7807	2
R3	UKPDS60	26.1196	QRISK3	21.4446	3
R4	UKPDS56	27.3467	UKPDS56	26.5499	4
R5	RRS	27.7954	RRS	26.8060	5
R6	NIPPON	31.8517	NIPPON	31.9123	6
R7	PROCAM	33.7465	PROCAM	33.7547	7
R8	WHO	33.8886	WHO	33.8951	8
R9	PCRS	34.3208	PCRS	34.3230	9
R10	SCORE	38.5167	SCORE	38.5167	10

*$MAD^N(CCVRC_n, \overline{AECRS1.0}_{10yr})$: Deviation of $CCVRC_n$ from.$\overline{AECRS1.0}_{10yr}$
*$MAD^N(AECRS1.\ 0_{10yr}, \overline{CCVRC}_n)$: Deviation of $AECRS1.\ 0_{10yr}$ from. $\overline{CCVRC}_n$

Appendix-Table 11
Ranking of the 10-year conventional cardiovascular risk calculators (CCVRCs) based on logistic regression and ROC analysis.

C1	C2	C3	C4	C5		C6	C7	C8		C9
R1	Calculator	OR	P-Val	OR 95% CI		AUC	P-Val	AUC 95% CI		Rank
				OR Lower	OR Upper			Lower AUC	Upper AUC	
R2	AECRS1.0$_{10yr}$	1.12	< 0.001	1.075	1.161	0.927	< 0.001	0.897	0.957	1
R3	QRISK3	1.06	< 0.001	1.03	1.081	0.884	< 0.001	0.839	0.929	2
R4	WHO	1.11	< 0.001	1.06	1.168	0.878	< 0.001	0.836	0.919	3
R5	PCRS	1.10	< 0.001	1.047	1.15	0.856	< 0.001	0.793	0.918	4
R6	FRS	1.04	< 0.001	1.017	1.061	0.834	< 0.001	0.768	0.899	5
R7	PROCAM	1.07	0.003	1.024	1.125	0.808	< 0.001	0.741	0.875	6
R8	UKPDS56	1.03	0.03	1.003	1.059	0.804	< 0.001	0.746	0.861	7
R9	RRS	1.02	0.18	0.992	1.044	0.789	< 0.001	0.725	0.853	8
R10	NIPPON	1.03	0.24	0.981	1.077	0.788	< 0.001	0.723	0.852	9
R11	UKPDS60	1.00	0.60	0.988	1.021	0.780	< 0.001	0.715	0.844	10
R12	SCORE	1.01	0.78	0.918	1.121	0.770	< 0.001	0.7	0.84	11

Appendix-Table 12
Proposed and international thresholds for risk stratification of patients into low-risk or high-risk class.

C1	C2	C3	C4	C5
#SN	Calculators	International Thresholds (%)	Proposed Thresholds (%)	Difference in Thresholds (%)
R1	FRS	20	20	0.0
R2	UKPDS56	20	20	0.0
R3	UKPDS60	20	20	0.0
R4	RRS*	10–20	10	10.0
R5	PCRS	7.5	7.5	0.0
R6	NIPPON*	5–10	5	5.0
R7	SCORE	5	5	0.0
R8	QRISK3*	10–20	10	0–10.0
R9	WHO	30	30	0.0
R10	PROCAM	20	20	0.0

*These calculator showed a range of values used in international threshold schemes. Difference zero indicates no difference between international threshold and our proposed thresholds.

References

[1] W.H. Organization, WHO Cardiovascular disease.
[2] J.-Y. Dong, Y.-H. Zhang, L.-Q. Qin, Erectile dysfunction and risk of cardiovascular disease, J. Am. Coll. Cardiol. 58 (2011) 1378.
[3] D. Prabhakaran, P. Jeemon, A. Roy, Cardiovascular diseases in India, Circulation 133 (2016) 1605–1620.
[4] P. Libby, P.M. Ridker, A. Maseri, Inflammation and atherosclerosis, Circulation 105 (2002) 1135–1143.
[5] A. Rosengren, S. Hawken, S. Ôunpuu, et al., Association of psychosocial risk factors with risk of acute myocardial infarction in 11 119 cases and 13 648 controls from 52 countries (the INTERHEART study): case-control study, Lancet 364 (2004) 953–962.
[6] M.J. O'Donnell, S.L. Chin, S. Rangarajan, et al., Global and regional effects of potentially modifiable risk factors associated with acute stroke in 32 countries (INTERSTROKE): a case-control study, Lancet 388 (2016) 761–775.
[7] G.M. Allan, S. Garrison, J. McCormack, Comparison of cardiovascular disease risk calculators, Curr. Opin. Lipidol. 25 (2014) 254–265.
[8] R.B. D'agostino, R.S. Vasan, M.J. Pencina, et al., General cardiovascular risk profile for use in primary care: the Framingham Heart Study, Circulation 117 (2008) 743–753.
[9] R.J. Stevens, V. Kothari, A.I. Adler, et al., The UKPDS risk engine: a model for the risk of coronary heart disease in Type II diabetes (UKPDS 56), Clin. Sci. 101 (2001) 671–679.
[10] V. Kothari, R.J. Stevens, A.I. Adler, et al., UKPDS 60: risk of stroke in type 2 diabetes estimated by the UK Prospective Diabetes Study risk engine, Stroke 33 (2002) 1776–1781.
[11] J. Hippisley-Cox, C. Coupland, P. Brindle, Development and validation of QRISK3 risk prediction algorithms to estimate future risk of cardiovascular disease: prospective cohort study, BMJ (2017) 357.
[12] P.M. Ridker, J.E. Buring, N. Rifai, et al., Development and validation of improved algorithms for the assessment of global cardiovascular risk in women: the Reynolds Risk Score, Jama 297 (2007) 611–619.
[13] N.D.R. Group, Risk assessment chart for death from cardiovascular disease based on a 19-year follow-up study of a Japanese representative population, Circ. J. 70 (2006) 1249–1255.
[14] R. Conroy, K. Pyörälä, A.e. Fitzgerald, et al., Estimation of ten-year risk of fatal cardiovascular disease in Europe: the SCORE project, Eur. Heart J. 24 (2003) 987–1003.
[15] W.H. Organization, Prevention of Cardiovascular Disease, World Health Organization2007.
[16] D.C. Goff, D.M. Lloyd-Jones, G. Bennett, et al., ACC/AHA guideline on the assessment of cardiovascular risk: a report of the American College of cardiology/American heart association Task Force on practice guidelines, J. Am. Coll. Cardiol. 63 (2013) 2935–2959 2014.
[17] G. Assmann, P. Cullen, H. Schulte, Simple scoring scheme for calculating the risk of acute coronary events based on the 10-year follow-up of the prospective cardiovascular Münster (PROCAM) study, Circulation 105 (2002) 310–315.
[18] W. Fan, Y. Ping, Association of Risk Factors for Cardiovascular Disease and Glomerular Filtration Rate: a Community-Based Study of 4925 Adults in Beijing vol. 97, Heart, 2011, p. A95.
[19] J.M. Sanches, A.F. Laine, J.S. Suri, Ultrasound Imaging, Springer2012.
[20] S. Zingg, T.-H. Collet, I. Locatelli, et al., Associations between cardiovascular risk factors, inflammation, and progression of carotid atherosclerosis among smokers, Nicotine Tob. Res. 18 (2015) 1533–1538.
[21] A. Laine, J.M. Sanches, J.S. Suri, Ultrasound Imaging: Advances and Applications, Springer2012.
[22] Y. Plantinga, S. Dogan, D.E. Grobbee, et al., Carotid intima-media thickness measurement in cardiovascular screening programmes, Eur. J. Cardiovasc. Prev. Rehabil. 16 (2009) 639–644.
[23] H. Øygarden, Carotid intima-media thickness and prediction of cardiovascular disease, Journal of the American Heart Association, 6 e005313.
[24] A. Kablak-Ziembicka, W. Tracz, T. Przewlocki, et al., Association of increased carotid intima-media thickness with the extent of coronary artery disease, Heart 90 (2004) 1286–1290.
[25] M.W. Lorenz, L. Gao, K. Ziegelbauer, et al., Predictive value for cardiovascular events of common carotid intima media thickness and its rate of change in individuals at high cardiovascular risk – results from the PROG-IMT collaboration, PLoS One 13 (2018) e0191172.

[26] E. Cuadrado-Godia, M. Maniruzzaman, T. Araki, et al., Morphologic TPA (mTPA) and composite risk score for moderate carotid atherosclerotic plaque is strongly associated with HbA1c in diabetes cohort, Comput. Biol. Med. 101 (2018) 128–145.
[27] E. Cuadrado-Godia, S.K. Srivastava, L. Saba, et al., Geometric total plaque area is an equally powerful phenotype compared with carotid intima-media thickness for stroke risk assessment: a deep learning approach, J. Vasc. Ultrasound (2018) 1544316718806421.
[28] J.H. Stein, C.E. Korcarz, R.T. Hurst, et al., Use of carotid ultrasound to identify subclinical vascular disease and evaluate cardiovascular disease risk: a consensus statement from the American Society of Echocardiography Carotid Intima-Media Thickness Task Force endorsed by the Society for Vascular Medicine, J. Am. Soc. Echocardiogr. 21 (2008) 93–111.
[29] V. Nambi, L. Chambless, A.R. Folsom, et al., Carotid intima-media thickness and presence or absence of plaque improves prediction of coronary heart disease risk: the ARIC (Atherosclerosis Risk in Communities) study, J. Am. Coll. Cardiol. 55 (2010) 1600–1607.
[30] J.H. Stein, H.M. Johnson, Carotid intima-media thickness, plaques, and cardiovascular disease risk: implications for preventive cardiology guidelines, J. Am. Coll. Cardiol. 55 (15) (2010) 1608–1610.
[31] J.F. Polak, M.J. Pencina, K.M. Pencina, et al., Carotid-wall intima-media thickness and cardiovascular events, N. Engl. J. Med. 365 (2011) 213–221.
[32] N. Ikeda, L. Saba, F. Molinari, et al., Automated carotid intima-media thickness and its link for prediction of SYNTAX score in Japanese coronary artery disease patients, Int. Angiol. 32 (2013) 339–348.
[33] N. Ikeda, A. Gupta, N. Dey, et al., Improved correlation between carotid and coronary atherosclerosis SYNTAX score using automated ultrasound carotid bulb plaque IMT measurement, Ultrasound Med. Biol. 41 (2015) 1247–1262.
[34] P. Lucatelli, E. Raz, L. Saba, et al., Relationship between leukoaraiosis, carotid intima-media thickness and intima-media thickness variability: preliminary results, Eur. Radiol. 26 (2016) 4423–4431.
[35] A. Gupta, K. Kesavabhotla, H. Baradaran, et al., Plaque echolucency and stroke risk in asymptomatic carotid stenosis: a systematic review and meta-analysis, Stroke 46 (2015) 91–97.
[36] M. Cesarone, G. Belcaro, A. Nicolaides, et al., Increase in echogenicity of echolucent carotid plaques after treatment with total triterpenic fraction of Centella asiatica: a prospective, placebo-controlled, randomized trial, Angiology 52 (2001) S19.
[37] J.D. Spence, M. Eliasziw, M. DiCicco, et al., Carotid plaque area: a tool for targeting and evaluating vascular preventive therapy, Stroke 33 (2002) 2916–2922.
[38] L. Lind, J. Sundström, J. Ärnlöv, et al., Impact of aging on the strength of cardiovascular risk factors: a longitudinal study over 40 years, Journal of the American Heart Association 7 (2018) e007061.
[39] K. Suastika, P. Dwipayana, M.S. Semadi, et al., Age Is an Important Risk Factor for Type 2 Diabetes Mellitus and Cardiovascular Diseases, Glucose Tolerance, Intech2012.
[40] M. Biswas, V. Kuppili, T. Araki, et al., Deep learning strategy for accurate carotid intima-media thickness measurement: an ultrasound study on Japanese diabetic cohort, Comput. Biol. Med. 98 (2018) 100–117.
[41] L. Saba, S.K. Banchhor, H.S. Suri, et al., Accurate cloud-based smart IMT measurement, its validation and stroke risk stratification in carotid ultrasound: a web-based point-of-care tool for multicenter clinical trial, Comput. Biol. Med. 75 (2016) 217–234.
[42] L. Saba, S.K. Banchhor, T. Araki, et al., Intra-and Inter-operator Reproducibility of Automated Cloud-Based Carotid Lumen Diameter Ultrasound Measurement, Indian Heart Journal, 2018.
[43] L. Saba, P.K. Jain, H.S. Suri, et al., Plaque tissue morphology-based stroke risk stratification using carotid ultrasound: a polling-based PCA learning paradigm, J. Med. Syst. 41 (2017) 98.
[44] T.J. Anderson, J. Grégoire, R.A. Hegele, et al., Update of the Canadian Cardiovascular Society guidelines for the diagnosis and treatment of dyslipidemia for the prevention of cardiovascular disease in the adult, Can. J. Cardiol. 29 (2012) 151–167 2013.
[45] N. Khanna, A. Jamthikar, T. Araki, et al., Nonlinear model for the carotid artery disease 10-year risk prediction by fusing conventional cardiovascular factors to carotid ultrasound image phenotypes: a Japanese diabetes cohort study, Echocadiography (2018) Accepted Article (In Production).
[46] L. Saba, G. Mallarini, R. Sanfilippo, et al., Intima Media Thickness Variability (IMTV) and its association with cerebrovascular events: a novel marker of carotid therosclerosis? Cardiovasc. Diagn. Ther. 2 (2012) 10.
[47] L. Saba, F. Molinari, K. Meiburger, et al., What is the correct distance measurement metric when measuring carotid ultrasound intima-media thickness automatically? Int. Angiol.: a journal of the International Union of Angiology 31 (2012) 483–489.
[48] F. Molinari, G. Zeng, J.S. Suri, A state of the art review on intima–media thickness (IMT) measurement and wall segmentation techniques for carotid ultrasound, Comput. Methods Progr. Biomed. 100 (2010) 201–221.
[49] F. Molinari, K.M. Meiburger, G. Zeng, et al., Automated carotid IMT measurement and its validation in low contrast ultrasound database of 885 patient Indian population epidemiological study: results of AtheroEdge™ Software, Int. Angiol. : a journal of the International Union of Angiology 31 (2012) 42–53.
[50] J.D. Spence, K. Solo, Resistant atherosclerosis: the need for monitoring of plaque burden, Stroke 48 (2017) 1624–1629.
[51] T. Rundek, J.D. Spence, Ultrasonographic measure of carotid plaque burden, JACC (J. Am. Coll. Cardiol.): Cardiovascular Imaging 6 (2013) 129.
[52] L. Saba, R. Montisci, F. Molinari, et al., Comparison between manual and automated analysis for the quantification of carotid wall by using sonography. A validation study with CT, EJR (Eur. J. Radiol.) 81 (2012) 911–918.
[53] F. Molinari, K.M. Meiburger, L. Saba, et al., Automated Carotid IMT Measurement and its Validation in Low Contrast Ultrasound Database of 885 Patient Indian Population Epidemiological Study: Results of AtheroEdge® Software, Multi-Modality Atherosclerosis Imaging and Diagnosis, Springer2014, pp. 209-219.
[54] G. Howard, A.R. Sharrett, G. Heiss, et al., Carotid artery intimal-medial thickness distribution in general populations as evaluated by B-mode ultrasound, ARIC Investigators, Stroke 24 (1993) 1297–1304.
[55] H.M. Johnson, P.S. Douglas, S.R. Srinivasan, et al., Predictors of carotid intima-media thickness progression in young adults: the Bogalusa Heart Study, Stroke 38 (2007) 900–905.
[56] K. Hansen, G. Östling, M. Persson, et al., The effect of smoking on carotid intima–media thickness progression rate and rate of lumen diameter reduction, Eur. J. Intern. Med. 28 (2016) 74–79.
[57] S.A. Rashid, S.A. Mahmud, Correlation between carotid artery intima-media thickness and luminal diameter with body mass index and other cardiovascular risk factors in adults, Sultan Qaboos University Medical Journal 15 (2015) e344.
[58] M. Duerden, N. O'Flynn, N. Qureshi, Cardiovascular risk assessment and lipid modification: NICE guideline, Br. J. Gen. Pract. 65 (2015) 378–380.
[59] W.A. Davis, S. Colagiuri, T.M. Davis, Comparison of the Framingham and United Kingdom prospective diabetes study cardiovascular risk equations in Australian patients with type 2 diabetes from the fremantle diabetes study, Med. J. Aust. 190 (2009) 180.
[60] H.-R. Ahn, M.-H. Shin, W.-J. Yun, et al., Comparison of the Framingham risk score, UKPDS risk engine, and SCORE for predicting carotid atherosclerosis and peripheral arterial disease in Korean type 2 diabetic patients, Korean journal of family medicine 32 (2011) 189–196.
[61] N.R. Cook, N.P. Paynter, C.B. Eaton, et al., Comparison of the Framingham and Reynolds Risk scores for global cardiovascular risk prediction in the multiethnic Women's Health Initiative, Circulation 125 (2012) 1748-S1711.
[62] M.C. Simmonds, N.J. Wald, Risk estimation versus screening performance: a comparison of six risk algorithms for cardiovascular disease, J. Med. Screen 19 (2012) 201–205.
[63] R.B. Manuel Santos, Jose Moura, Mariano Pego, ACC/AHA 2013 and SCORE CV Risk Calculators: Are They the Same in a Low-Risk Southern European Population? American College of Cardiolog, American College of Cardiology: Expert Analysis, 2015.
[64] A. Dalton, A. Bottle, M. Soljak, et al., The comparison of cardiovascular risk scores using two methods of substituting missing risk factor data in patient medical records, J. Innovat. Health Inf. 19 (2011) 225–232.
[65] E. Alemao, H. Cawston, F. Bourhis, et al., Comparison of cardiovascular risk algorithms in patients with vs without rheumatoid arthritis and the role of C-reactive protein in predicting cardiovascular outcomes in rheumatoid arthritis, Rheumatology 56 (2017) 777–786.
[66] N. Garg, S.K. Muduli, A. Kapoor, et al., Comparison of different cardiovascular risk score calculators for cardiovascular risk prediction and guideline recommended statin uses, Indian Heart J. 69 (2017) 458–463.
[67] D. Bansal, R.S. Nayakallu, K. Gudala, et al., Agreement between Framingham risk score and United Kingdom Prospective Diabetes Study risk engine in identifying high coronary heart disease risk in North Indian population, Diabetes & metabolism journal 39 (2015) 321–327.
[68] S. Selvarajah, G. Kaur, J. Haniff, et al., Comparison of the Framingham Risk Score, SCORE and WHO/ISH cardiovascular risk prediction models in an Asian population, Int. J. Cardiol. 176 (2014) 211–218.
[69] N.J. Bosomworth, Practical use of the Framingham risk score in primary prevention: Canadian perspective, Canadian family physician Medecin de famille canadien 57 (2011) 417–423.
[70] N.R. Cook, N.P. Paynter, C.B. Eaton, et al., Comparison of the Framingham and Reynolds Risk scores for global cardiovascular risk prediction in the multiethnic Women's Health Initiative, Circulation, CIRCULATIONAHA 111 (2012) 075929.
[71] NICE, Cardiovascular Disease: Risk Assessment and Reduction, Including Lipid Modifification, (2014).
[72] W.T.f. Encyclopedia, Sample (Statistics), (2018).
[73] L. Saba, S.K. Banchhor, N.D. Londhe, et al., Web-based accurate measurements of carotid lumen diameter and stenosis severity: an ultrasound-based clinical tool for stroke risk assessment during multicenter clinical trials, Comput. Biol. Med. 91 (2017) 306–317.
[74] T. Araki, N. Ikeda, D. Shukla, et al., PCA-based polling strategy in machine learning framework for coronary artery disease risk assessment in intravascular ultrasound: a link between carotid and coronary grayscale plaque morphology, Comput. Methods Progr. Biomed. 128 (2016) 137–158.
[75] F. Molinari, G. Zeng, J.S. Suri, Intima-media thickness: setting a standard for a completely automated method of ultrasound measurement, IEEE Trans. Ultrason. Ferroelectrics Freq. Contr. 57 (2010) 1112–1124.
[76] J.S. Suri, C. Kathuria, F. Molinari, Atherosclerosis Disease Management, Springer Science & Business Media2010.
[77] F. Molinari, G. Zeng, J.S. Suri, A state of the art review on intima-media thickness (IMT) measurement and wall segmentation techniques for carotid ultrasound, Comput. Methods Progr. Biomed. 100 (2010) 201–221.
[78] F. Molinari, K.M. Meiburger, L. Saba, et al., Ultrasound IMT measurement on a

multi-ethnic and multi-institutional database: our review and experience using four fully automated and one semi-automated methods, Comput. Methods Progr. Biomed. 108 (2012) 946–960.

Narendra N. Khanna, MD, DM, FACC is Advisor to Apollo Group of Hospitals in India and is working as Senior Consultant in Cardiology & Coordinator of Vascular Services at Indraprastha Apollo Hospital, New Delhi.

Ankush D. Jamthikar, M.Tech. has received MTech in Communication System and currently working as PhD research scholar at Visvesvaraya National Institute of Technology, Nagpur, India.

Deep Gupta, PhD is an Assistant Professor in the Electronics & Communication Engineering Department, VNIT, Nagpur (India). He received his Ph.D. in Medical Image Processing form Indian Institute of Technology Roorkee, India.

Andrew Nicolaides, MS, FRCS, PhD (Hon) is currently the Professor Emeritus at Imperial College, London. He is the co-author of more than 500 original papers and editor of 14 books.

Tadashi Araki, MD received the MD degree from Toho University, Japan in 2003. His research topics include coronary intervention, intravascular ultrasound (IVUS) and peripheral intervention.

Luca Saba, MD is with A.O.U. Cagliari, Italy. His research interests are in Multi-Detector-Row Computed Tomography, Magnetic Resonance, Ultrasound, Neuroradiology, and Diagnostic in Vascular Sciences.

Dr. Elisa Cuadrado Godia, Ph. D., is with IMIM – Hospital del Mar, Passeig Marítim 25–29, Barcelona, Spain. She works with Neurovascular Research Group and her current research interests are in the field of carotid artery disease and cardio vascular diseases.

Aditya Sharma, MD is a cardiologist at University of Virginia, where he directs the anticoagulation clinic and the medical optimization clinic, which helps patients with vascular disorders manage their risk factors with medication. His research interests are Peripheral arterial disease, venous thromboembolism, and fibromuscular dysplasia.

Tomaz Omerzum, MD is currently working as at University Medical Centre Maribor, Slovenia. His Research interests are radiology, and cardiovascular medicine.

Harman S. Suri is currently pursuing his BS from Brown University, Providence, RI, USA. He worked in summers of 2015 in the area of telemedicine-based Autism industry at Behavioral Imaging, Boise, Idaho, USA.

Ajay Gupta, MD, MS currently working as associate professor of radiology and neuroscience at Weil Cornell Medical College New York, USA. His research is focused on neuroradiology.

Sophie Mavrogeni, MD, PhD currently working at Cardiology Clinic, Onassis, Athens, GREECE. Her research is focused on Non-ischemic Cardiomyopathy, Dystrophinopathies, myocarditis and rheumatic diseases.

Monika Turk, MD is currently working as Physician at Department of Neurology, University Medical Centre Maribor, Maribor, Slovenia.

John R. Laird, MD, FACC is with St. Helena Hospital, CA, USA. Professor Laird is an internationally renowned interventional cardiologist and his expertise is innovative procedures for carotid artery disease.

Athanasios Protogerou, MD, PhD currently working at the Department of Cardiovascular Prevention & Research Unit Clinic, National and Kapodistrian Univ. of Athens, GREECE. His research is focused on Cardiovascular prevention.

Petros P. Sfikakis, MD, is the Dean of the School of Medicine at National and Kapodistrian University of Athens, Greece, and a Professor of Internal Medicine and Rheumatology. One of his main research interest focus in the cardiovascular outcomes of patients with immune-mediated diseases.

George D. Kitas, MD, PhD, FRCP is director of Research & Development-Academic Affairs, Dudley Group NHS Foundation Trust, Dudley, UK. He is an Honorary Professor of Rheumatology at the Arthritis Research UK Epidemiology Unit.

Vijay Viswanathan MD, PhD, FRCP is currently working as a chairman and director of MV Hospital for Diabetes and M Viswanathan Diabetes Research Centre, Chennai, India. His Research interests are Endocrinology Diabetes and Metabolism, Diabetes and foot research.

Jasjit S. Suri, Ph.D., MBA, Fellow AIMBE is with AtheroPoint™, Roseville, CA, USA. He is an innovator, visionary, scientist and an internationally known world leader in the field of biomedical imaging. Dr. Suri is a recipient of Marquis Life Time Achievement Award.